

RATE LIMITED DIFFUSION AND DISSOLUTION OF MULTI-COMPONENT
NON-AQUEOUS PHASE LIQUIDS (NAPLS)
IN GROUNDWATER

by

WILLIAM RANDOLPH BURKE, JR

GEOFFRY R. TICK, COMMITTEE CHAIR
RONA J. DONAHOE
YUEHAN LU
MARLON R. COOK

A THESIS

Submitted in fulfillment of the requirements
for the degree of Master of Science
in the Department of Geological Sciences
in the Graduate School of
The University of Alabama

TUSCALOOSA, ALABAMA

2012

Copyright William Randolph Burke, Jr. 2012

ALL RIGHTS RESERVED

ABSTRACT

Contamination of soil and groundwater by nonaqueous phase liquids (NAPLs) poses serious risks to human health and the environment and presents major challenges for cleanup. The presence of complex NAPL mixtures in the subsurface further complicates remediation efforts, transport predictions, and the development of accurate risk assessments. A comprehensive laboratory-scale study was conducted to elucidate the factors affecting dissolution and removal of NAPL including 1) the distribution of NAPL (uniform vs. non-uniform), 2) NAPL-water interfacial area (constant vs. changing), 3) multi-component NAPL systems (composition dependence), and 4) intra-NAPL diffusion. A series of column and time sequential batch experiments were conducted to assess the factors controlling dissolution processes under dynamic flow and equilibrium conditions. For comparison purposes, two independent NAPL systems were established for the series of experiments including single-component trichloroethene (TCE) whereby the NAPL interfacial area decreases as dissolution proceeds, and two-component TCE-hexadecane (HEX) in which the bulk NAPL (comprised primarily of insoluble HEX) interfacial remains constant. The results of this study show that significant dissolution rate and removal limitations during water-flushing exist for systems containing non-uniform NAPL (TCE) distributions, due to less available NAPL-water interfacial area. Effective TCE removal was 2 times longer for the non-uniform NAPL distribution experiment. TCE dissolution in the two-component NAPL systems (TCE and HEX) experienced significantly less rate limitation (absence of concentration tailing) than the single-component TCE systems due to the presence of a constant interfacial area for mass-transfer to occur during flushing. Each column experiment resulted in differing effectiveness with respect to mass

removal. The multi-component TCE:HEX system experienced the fastest mass removal time, but was not considered the most efficient. The batch experiments demonstrated that as mole fraction of a particular component of a NAPL (TCE) mixture decreases, greater dissolution nonideality occurs, resulting in greater observed concentrations than those predicted by equilibrium dissolution (i.e. Raoult's Law). Dissolution nonideality, quantified by the NAPL-activity coefficient, increased for the lower TCE mole fraction systems from 1.7 to 6.1 for TCE:HEX mole fractions of 0.2:0.8 to 0.003:0.997, respectively. The results of the batch experiments also indicate that dissolution mass-transfer rates were nearly identical for both the single-component TCE systems and the TCE:HEX systems. This suggests that intra-NAPL diffusion is not a rate-limited process under the conditions of these experiments. Mass flux reduction analyses showed that the two-component (TCE:HEX) NAPL experiment resulted in less efficient removal behavior than the single-component TCE flushing experiments, likely due to the significantly lower TCE mass within the mixed NAPL system. The results from this study improved the understanding of NAPL dissolution and removal processes; most notably for NAPL mixture systems where NAPL-water interfacial area may be maintained during flushing and where significant dissolution nonideality may result from decreasing mole fractions of target contaminants in NAPL.

LIST OF ABBREVIATIONS AND SYMBOLS

cm	Centimeter
γ	Gamma
hr	hour
I.D.	Inner diameter
L	Liter
min	Minute
mg	Milligram
mL	Milliliter
nm	Nanometer
S_N	Saturation: a condition in which a quantity no longer responds to some external influence
q	Darcy's velocity (L/T)
T	Time
UV	Ultraviolet: wavelengths shorter than light but longer than X-rays
V_p	Linear pore velocity
wt%	Weight percent
%	Percent
>	Greater than
\pm	Plus or Minus
Σ	Summation: The arithmetic operation of calculating the sum of two or more numbers
=	Equal to

ACKNOWLEDGMENTS

I would like to thank my advisor, Dr. Tick, for his encouragement and dedication.

I would also like to thank my friends and family for their continuous support.

CONTENTS

<u>ABSTRACT</u>	ii
<u>LIST OF ABBREVIATIONS AND SYMBOLS</u>	iv
<u>ACKNOWLEDGMENTS</u>	v
<u>LIST OF TABLES</u>	viii
<u>LIST OF FIGURES</u>	ix
<u>CHAPTER 1. INTRODUCTION AND MOTIVATION</u>	1
<u>Introduction</u>	1
<u>Motivation</u>	3
<u>CHAPTER 2. BACKGROUND AND LITERATURE REVIEW</u>	7
<u>Background</u>	7
<u>Literature Review</u>	14
<u>CHAPTER 3. RATE LIMITED DIFFUSION AND DISSOLUTION OF MULTI- COMPONENT NON-AQUEOUS PHASE LIQUIDS (NAPLS) IN GROUNDWATER</u>	19
<u>Introduction</u>	19
<u>Materials and Methods</u>	19
<u>Results</u>	32
<u>Discussion</u>	51
<u>Ideal and Non-Ideal Dissolution Modeling</u>	65
<u>CHAPTER 4. CONCLUSION</u>	77
<u>REFERENCES</u>	86

LIST OF TABLES

<u>Table 1: Pertinent media properties (20/30 mesh quartz sand)</u>	20
<u>Table 2: Pertinent NAPL properties (TCE and Hexadecane)</u>	21
<u>Table 3: Peclet Numbers from conservative tracer tests</u>	25
<u>Table 4: Column Conditions : Pore Volume and Residual Saturation</u>	26
<u>Table 5: Column Conditions : Flow Direction under specific Conditions</u>	27
<u>Table 6: TCE Dissolution Rates for static equilibrium experiments</u>	64
<u>Table 7: TCE:Hexadecane- Column experiment conditions</u>	68

LIST OF FIGURES

<u>Figure 1: Schematic representation of intra-NAPL diffusion with NAPL dissolution</u>	7
<u>Figure 2: Mass flux reduction relationships from the dissolution of immiscible liquids in porous media</u>	13
<u>Figure 3: Schematic of experimental set-up</u>	30
<u>Figure 4: TCE elution curve (uniformly packed conditions)</u>	34
<u>Figure 5: TCE mass flux reduction (uniformly packed conditions)</u>	35
<u>Figure 6: Normalized TCE mass removal (uniformly packed conditions)</u>	36
<u>Figure 7: TCE elution curve (non-uniformly packed conditions)</u>	39
<u>Figure 8: TCE mass flux reduction (non-uniformly packed conditions)</u>	40
<u>Figure 9: Normalized TCE mass removal (non-uniformly packed conditions)</u>	42
<u>Figure 10: TCE:Hexadecane elution curve (uniformly packed conditions)</u>	44
<u>Figure 11: TCE:Hexadecane mass flux reduction (uniformly packed conditions)</u>	45
<u>Figure 12: Normalized TCE:Hexadecane mass removal (non-uniformly packed conditions)</u>	46
<u>Figure 13: TCE equilibrium time series dissolution</u>	48
<u>Figure 14: TCE:Hexadecane (0.2: 0.8 volume fraction) time series dissolution</u>	49
<u>Figure 15: TCE:Hexadecane (0.003: 0.997) volume fraction) time series dissolution</u>	51
<u>Figure 16: TCE elution curves for all column experiments</u>	59
<u>Figure 17: Mass flux reduction of TCE for all column experiments</u>	60
<u>Figure 18: Normalized TCE mass recovery for all column experiments</u>	61
<u>Figure 19: Three dimensional representations of TCE and Hexadecane</u>	66

Figure 20: TCE:Hexadecane - Observed TCE concentration vs. equilibrium prediction without gamma adjustment.....69

Figure 21: TCE:Hexadecane- TCE mole fraction vs. Pore volume flushed.....71

Figure 22: TCE:Hexadecane- Observed TCE concentration vs. equilibrium prediction with gamma adjustment.....73

CHAPTER 1: Introduction and Motivation

Introduction

Current and previous hazardous waste disposal practices have become an important facet of environmental regulatory criteria due to the widespread prevalence of sites contaminated by multiple chemicals and complex mixed-waste systems, as hazardous waste disposal sites incorporate multiple contaminants from multiple locations. Improper handling and disposal, spills, and leaking of underground storage tanks (UST) can also introduce dangerous chemicals into the environment, including both single and multi-component contaminant phases (Zhang et al., 2007) Hazardous waste disposal sites and many other contaminated sites commonly contain various compounds (e.g., McCray and Dugan, 2002; Rao et al., 1997; McCray and Brusseau, 1998; McCray et al., 2011) ranging from light non-aqueous phase liquids (LNAPLs) and petroleum hydrocarbon derivatives (i.e. decane) to dense non-aqueous phase liquids (DNAPLs) such as chlorinated solvents (i.e. TCE), and mixtures of both immiscible liquids and miscible liquids. The presence of immiscible liquids within the subsurface is the single most important factor limiting cleanup of soil and groundwater (NRC 2005). This is in part due to the fact that immiscible liquids commonly become trapped as “residual saturation” within the subsurface and cannot be easily displaced, thereby presenting a long-term source of contamination to groundwater. In addition, immiscible liquids typically have extremely low aqueous solubilities and therefore contaminant removal is dependent upon the slow rate kinetics associated with dissolution. In other words, the trapped immiscible liquid source zones must dissolve into the water (i.e. groundwater) to effectively remove through pump and treat or chemical flushing

methods, which can be an extremely slow process. Since aqueous solubilities of these immiscible liquid compounds are low, a very small fraction of the contaminant mass can readily dissolve into the aqueous phase (groundwater). The dissolution and remediation process is further complicated by systems in which there are multiple components and chemical mixtures comprising the immiscible liquid contamination. Furthermore, the chemicals associated with these immiscible liquid contaminants are typically extremely toxic to humans and the environment. Many of these compounds are classified as carcinogens or suspect carcinogens, teratogens, and mutagens. Combinations of multi-component organic compounds pose a significant threat to the quality of water resources and potential drinking water sources due to the relatively low solubility by themselves, but in conjunction with other compounds, the low solubility can be further enhanced, resulting in years or decades of groundwater contamination (Brahma and Harmon, 2003; Zhang et al., 2007). As the variety of chemicals differs from location to location, as well as within individual locations, the extent of a NAPL's (either single or multi-component) behavior can become non-ideal and anomalous. Such variant compounds have distinct chemical and physical characteristics, but in conjunction with each other can result in complicated behavior that is poorly understood, which can lead to inaccurate risk assessment, poor prediction of contaminant transport, and improper remediation design.

In addition to the complex behavior of multi-component systems, the presence of heterogeneous NAPL distributions within the subsurface can complicate dissolution processes, limit remediation effectiveness, and challenge predictions and understanding of contaminant transport behavior. NAPL distributed unevenly throughout a system can drastically inhibit site characterization and remediation, as high residual NAPL "pools" can collect in receptive locations becoming hydraulically inaccessible to flow and thereby altering NAPL dissolution

behavior (Werner et al., 2009). NAPL source zone architecture greatly influences contaminant transport behavior as variations in grain type, size, and texture can generate preferential flow paths, further limiting understanding and predictability of contaminant transport (Illangasekare et al., 1995; Zhang et al., 2007). Because subsurface heterogeneity and variability is complex at most sites, it is expected that multiple-component immiscible liquid contamination will result in dynamic and highly complicated contaminant transport behavior. A better understanding of contaminant transport and effects related to immiscible liquid distribution can be invaluable to the development of more effective remediation strategies, characterization methods, and risk assessments for sites contaminated by a wide variety of NAPLs and subsurface heterogeneity.

The purpose of this study was to evaluate the dependency and relationship of immiscible liquid interfacial area on dissolution behavior of a chlorinated compound established within a physically homogeneous porous medium. A series of column experiments were designed to elucidate how constant versus changing interfacial area affect dissolution processes. A series of batch experiments were conducted to examine dissolution and diffusion processes under equilibrium conditions. Lastly, the study compared mass removal and mass flux relationships for systems in which the immiscible liquid interfacial area decreased during flushing to those systems whereby the immiscible liquid interfacial area remained essentially constant during flushing.

Motivation

Some of the most problematic contaminants, in terms of removal and toxicity, are associated with the release of non-aqueous phase liquids (NAPLs) into the environment. The presence of immiscible organic liquids is generally considered to be the single most important factor limiting remediation of sites contaminated by organic compounds (NRC 1999, 2000,

2005). These types of contaminants are found as fuel oils, gasolines, and cleaning solvents. Due to the recalcitrant nature of these types of chemicals, appropriate measures must be taken for their disposal. Common sources of groundwater contamination include underground storage tanks where petroleum type hydrocarbons are stored at fuel stations and solvents (i.e. TCE and PCE) are used in various degreasing/cleaning and/or manufacturing processes which are subject to leakage. Improper installation and corrosion of underground storage tanks are prime culprits of such contaminant release (Carroll 2007). Landfills or hazardous waste disposal sites are also sources for NAPLs which have migrated, diffused and/or leached into the subsurface. According to the U.S. Environmental Protection Agency in 1991, 63% of hazardous waste sites surveyed reported detecting NAPLs or NAPL-derived constituents in monitoring wells, surface water and/or soil (Haebeck, 1994). Surveys reporting such a large quantity of incidents indicate the immediacy of remediating these types of contaminants from the subsurface. Remediation effectiveness will depend on a number of factors, including the rate of NAPL dissolution which is a primary factor limiting cleanup.

The presence of complex multi-component NAPL mixtures further complicates the remediation process (McCray and Brusseau, 1998, 1999). Very seldom is any particular contamination site affected by a single contaminant (Mercer and Cohen, 1990). The dissolution and diffusion of components within bulk immiscible liquid (NAPL) mixtures can behave very differently than systems that are contaminated by single-component NAPLs. The occurrence of multiple contaminants is directly relevant in the case of organic immiscible liquids, particularly petroleum hydrocarbons and derivatives, due to their similar chemical composition and structure (Zemo et al., 1993). Petroleum hydrocarbons and derivatives are composed of carbon and hydrogen atoms and are obtained from various fossil fuels such as crude oil, gasoline, natural

gas, and coal (Schwartz and Zhang, 2003). Other ubiquitous immiscible liquid types of contamination include the class of chlorinated solvents such as dichloroethene, trichloroethene, and tetrachloroethene. When considering the relevance of the hydrocarbon's original source, it may be appropriate to assume their congruent occurrence in natural systems; however, in many cases a host of contaminants can comprise complex mixtures occurring from different and varied industrial/commercial sources. With a multi-component NAPL, an eclectic variety of chemical properties can be present (Geller and Hunt, 1993). These complex mixtures tend to enhance the uncertainty of NAPL behavior as the variety of properties within the total NAPL mixture can be resultant of many individual NAPL properties. For example, when considering overall solubility of a NAPL mixture, one has to take into consideration the individual solubility's of each component of the bulk NAPL mixture. However, when certain components within the bulk NAPL exhibit contradictory properties or vastly different structure or characteristics (i.e. soluble vs. insoluble; chained vs. aromatic, etc.) the importance of understanding the influence of contributing factors to multi-component immiscible liquid dissolution behavior becomes much more evident. Thus, one primary contributing factor present in the case of a multi-component mixture containing both soluble and insoluble components is the NAPL-water interfacial surface area.

It is also important to note the conditions under which a NAPL is released in order to understand its ultimate transport behavior. While it is easily accepted that many lab experiments utilize homogeneous subsurface conditions in order to isolate one, or few, variables, a handful of experiments attempt to tackle more complex subsurface conditions. There have been approaches such as increasing heterogeneity by incorporating different grain sizes and size fractions within flow cells (Zhang et al., 2007) whereby more hydraulically conductive zones are implemented

resulting in preferential flow paths. A study conducted by Zhang et al. (2007) indicated that the presence of preferential flow paths led to subsequent preferential NAPL dissolution under the conditions of their experiments. While there may be a constant groundwater flow in isolated zones of contamination, a NAPL plume may dissolve at different rates due to preferential flow paths within a groundwater system. Thus, since NAPL dissolution is dependent on how much surface area is present, the presence of preferential flow paths, and variations of contaminant concentration within bulk aqueous phase plume, resulting NAPL dissolution may not behave as previously predicted. Also, specific distribution and architecture of NAPL ganglia and pools have been observed to significantly affect the rate of resulting dissolution. In particular, ganglia can exist under extremely high saturations or “pools” whereby the groundwater is limited to the associated reduced NAPL-water interfacial area. Because these highly saturated NAPL ganglia or pools essentially fill the entire pore space, the groundwater is forced to by-pass the NAPL source due to the reduced-permeability within that region (i.e. NAPL bypass flow). NAPL source zones can also exist as residual saturation whereby the immiscible fluid redistributes within the subsurface under relatively low saturation becoming trapped in place by strong resulting capillary forces. These residual saturation zones may not reduce the in-situ permeability as significantly as NAPL “pools,” but they still reduce the in-situ permeability within that region causing NAPL bypass flow and abnormal dissolution kinetics (Brusseau et al., 2002).

CHAPTER 2: Background and Literature Review

Background

Diffusion is the process by which molecular species move from areas of high concentration to areas of low concentration. Movement is random and tends to distribute particles more uniformly (Wilson and Moore, 1998). A schematic of the diffusion process is exemplified in Figure 1.

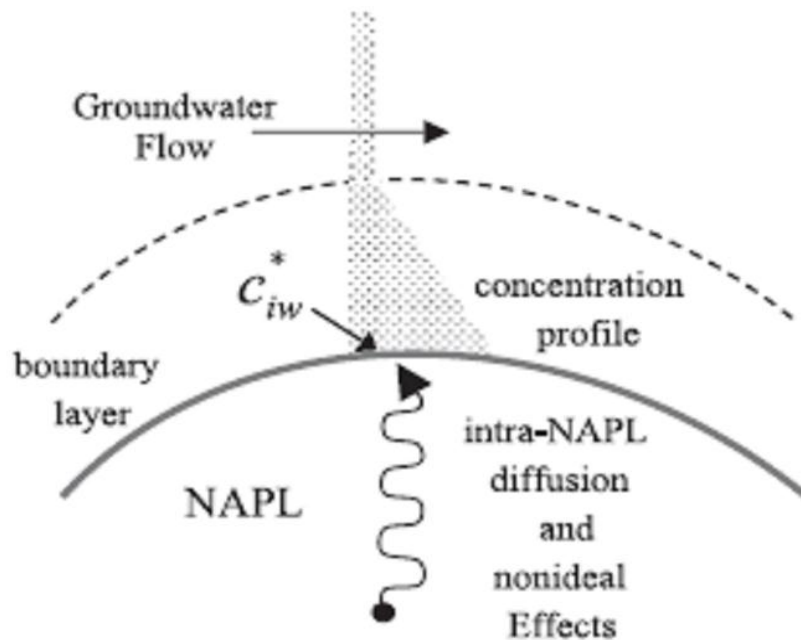


Figure 1. Schematic representation of intra-NAPL diffusion with NAPL dissolution (adapted from Frind et al., 1999).

This study examined dissolution and diffusion transport processes as a function of NAPL/water interfacial area and the effect of intra-NAPL diffusion on dissolution rates within

multi-component NAPL/groundwater systems. Intra-NAPL diffusion processes were evaluated through time-sequential batch experiments. The properties of the contaminants allowed for a unique opportunity to study the diffusion of one NAPL component through another without decreasing the overall bulk NAPL specific surface area because of negligible dissolution of the bulk NAPL (n-hexadecane). The sequential time batch experiments were evaluated using the equilibrium multi-component dissolution (mass-transfer) relationships described by Raoult's Law. Raoult's Law describes the equilibrium partitioning behavior between the NAPL mixture and the aqueous water phase. Raoult's Law is described herein by:

$$C_A = C_S x_i^N \gamma_i^N \quad (1)$$

where C_A represents the dissolved phase concentration of component i from the NAPL mixture, x_i^N represents the mole fraction of component i of the NAPL mixture, C_S is the single-component aqueous solubility of component i of the NAPL mixture, and γ_i^N is the activity coefficient of component i of the NAPL mixture which describes the effects of "non-ideal" partitioning. The γ_i^N term may be larger than unity (NAPL phase non-ideal condition) when the organic chemical is significantly dissimilar in shape, size, or polarity from the average characteristics of the bulk NAPL mixture, especially when the NAPL phase mole fraction of the constituent is small (Banerjee, 1984; Burris and MacIntyre, 1985; Schwarzenbach et al., 1993). Concentrations were evaluated over time to assess differences in dissolution rates between the single-component NAPL contaminant and the TCE:Hexadecane mixed NAPL system, as well as observing the ideality of each NAPL composition.

Dissolution is the process of dissolving into a homogenous aqueous solution (Wilson and Moore, 1998). The governing equation for solute transport with dissolution of immiscible liquid is given by (e.g., Zhang and Brusseau, 1999):

$$\theta_a \frac{\partial C}{\partial t} + \rho_N \frac{\partial \theta_N}{\partial t} = \frac{\partial}{\partial x} \left(\theta_a D \frac{\partial C}{\partial x} \right) - q \frac{\partial C}{\partial x} \quad (2)$$

where C is the aqueous concentration of solute; θ_a is the fractional volumetric water content; θ_N is the fractional volumetric content of the immiscible liquid phase; ρ_N is the density of the immiscible liquid; q is the Darcy velocity through the column; D is the dispersion coefficient; x is the Cartesian coordinate in one-dimension; and t is time. Sorption of TCE by the porous medium used in these experiments is negligible, and is therefore ignored. Immiscible-liquid dissolution is described with the widely used first-order mass transfer equation (Miller et al., 1990; Powers et al., 1992, 1994; Imhoff, et al., 1994):

$$\rho_N \frac{\partial \theta_N}{\partial t} = k_f a^0 (C_s - C) \quad (3)$$

where k_f [LT^{-1}] is the local mass transfer rate coefficient for dissolution, a^0 [L^2L^{-3}] is the specific surface area of the NAPL/water interface and C_s is the aqueous solubility of the immiscible liquid. Rates of dissolution were evaluated in systems by which interfacial areas of the NAPL/water changes over time (single-component) and for systems by which the interfacial area of the NAPL/water remains constant (multi-component). In the systems with a constant NAPL/water interfacial area, dissolution primarily occurs as a function of the local mass transfer coefficient in contrast to the changing NAPL/water interfacial area which can be attributed to both interfacial area reduction and resulting effects on the local mass transfer coefficient for the single-component NAPL systems. These transport processes are critical to understanding rate

limited diffusion and effects on dissolution so that more effective remediation and more accurate risk assessments can be developed.

Mass flux is the rate of contaminant mass flow over a unit area or boundary. As a NAPL enters the subsurface, the dissolution process begins as small fractions of the bulk NAPL begin to enter the aqueous phase. Even minute concentrations of dissolved NAPL can contaminate immense quantities of groundwater (TCE solubility: 1200 ppm; TCE Maximum Contaminant Level: 5 ppb). With the difficulty of subsurface characterization, apparent aqueous concentrations can vary from location to location as NAPL may be trapped in pools, misdirecting the site characterization process. Thus, aqueous concentrations are not direct indicators of actual mass being removed from a contaminated site. Mass flux is controlled by a variety of variables, including source zone architecture and NAPL distribution (Soga et al., 2004). These limiting factors directly influence the rate of reduction of mass during remediation of a contaminated site. Homogeneously distributed NAPL in homogeneous subsurface conditions are more conducive to contaminant removal with respect to adverse (i.e. non-ideal) conditions. Conversely, pooled NAPL and heterogeneous subsurface conditions inhibit mass removal. Mass flux reduction (MFR) assesses the rate by which mass (i.e. NAPL) is reduced/removed relative to cumulative mass removed. MFR is defined as,

$$MFR = 1 - \frac{J_f}{J_i} = 1 - \frac{Q_f C_f}{Q_i C_i} \quad (4)$$

where J is the mass flux (M / T^{-1}), Q is the volumetric flow rate (L / T^{-1}), C is concentration (M / L^{-3}), and the subscripts i and f represent initial and final, respectively. The above expression (Eq. 4) simplifies to the following equation if volumetric flow rate is held constant during the measurements:

$$MFR = 1 - \frac{C_f}{C_i} \quad (5)$$

Many studies have generally categorized mass flux behavior as ideal or non-ideal based on the degree of heterogeneity of the porous medium and/or by the distribution of NAPL in the system (Enfield et al., 2002; Parker and Park, 2004; NRC, 2005; Marble et al., 2008; Carroll and Brusseau, 2009). Resulting contaminant mass flux from the dissolution of immiscible liquid can be significantly limited in a heterogeneous system as non-uniform distribution of contaminant limits the dissolution process (Tick and Rincon, 2009). Under ideal conditions, optimum mass can be removed during most of the dissolution process. Thus, mass flux remains essentially constant, and at the optimal level. However, as increased dissolution occurs, less mass can be removed and mass flux is reduced. This is due to interfacial surface area reaching a critical point whereby maximum mass transfer conditions are no longer present, thus reducing the most favorable mass flux conditions. However, if more non-ideal conditions are in place, linear or erratic behavior may be observed and mass flux reduction-cumulative mass reduction relationships will follow non-ideal behavior in which the mass flux is reduced quickly before significant mass has been depleted (Figure 2. A). It is accepted that under heterogeneous subsurface conditions, contaminant transport processes exhibit non-ideal behavior (mass removal characteristics) compared with homogeneous subsurface conditions. Assessment of the importance of NAPL characterization (i.e. NAPL distribution, NAPL-water interfacial area, porous medium packing) is paramount for the understanding the impact of dissolution, mass flux, and mass removal behavior of these systems. This research evaluates the effect of changing NAPL-water interface on mass flux reduction during dissolution flushing and also evaluates mass flux reduction effects due to “heterogeneous” subsurface conditions through uniform and

non-uniform porous medium packing methods (i.e. uniform vs. non-uniform NAPL distribution).

A mass removal function (Tick and Rincon, 2009) was used to construct a model describing the efficiency of contaminant removal which can be applied to estimate the relationship between MFR and mass removal. The function is as follows,

$$1 - \frac{J_f}{J_i} = \left(1 - \frac{M_f}{M_i} \right)^{1/n} \quad (6)$$

where M is source zone mass and n is a fitting parameter. This fitting parameter, n , describes the relationship between mass flux reduction (MFR) and actual mass removal as a function of flow field dynamics, mass transfer processes, and specific removal dynamics associated with the solubilization agent (i.e. water) itself. Values for n are indicative of the ideality of mass flux reduction. For values $n > 1$, mass flux reduction begins increasing quickly before a significant fraction of the mass is removed (i.e. non-ideal conditions or inefficient mass removal). The opposite holds true for values $n < 1$. These values represent maximum mass flux is maintained for extended periods of flushing allowing for increased mass removal (i.e. ideal conditions; Figure 2 B). Similar mass removal approaches have been used to examine NAPL removal and resulting mass flux behavior (Rao et al. 2002; Zhu and Sykes 2004; Falta et al. 2005; Jawitz et al. 2005; Brusseau et al. 2008; DiFilippo and Brusseau et al. 2008).

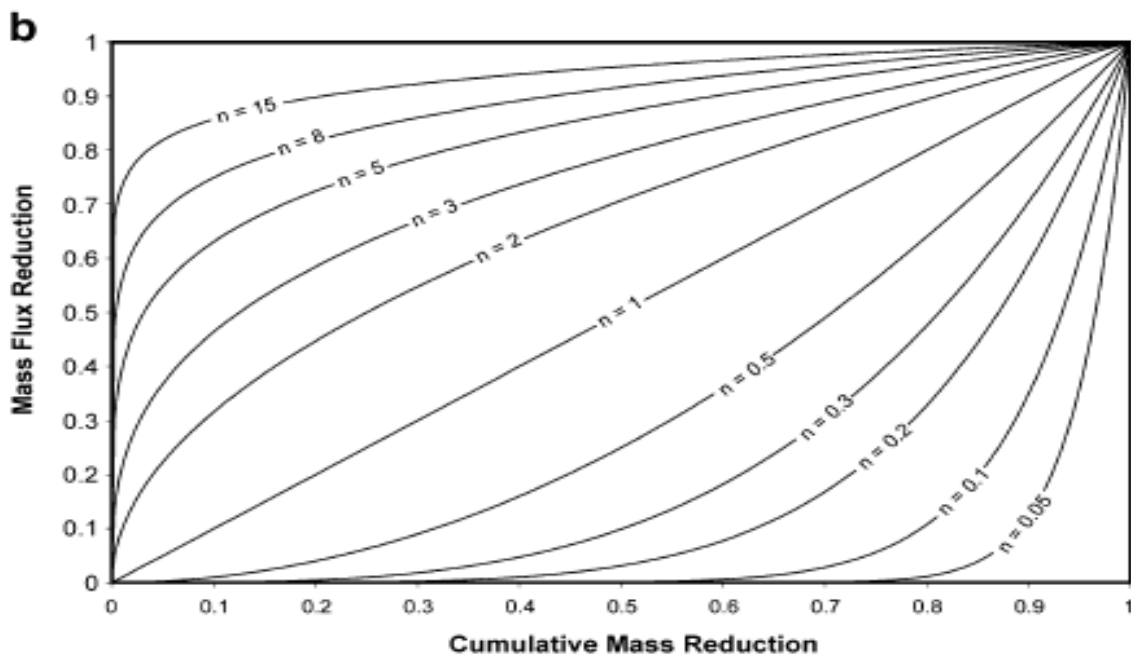
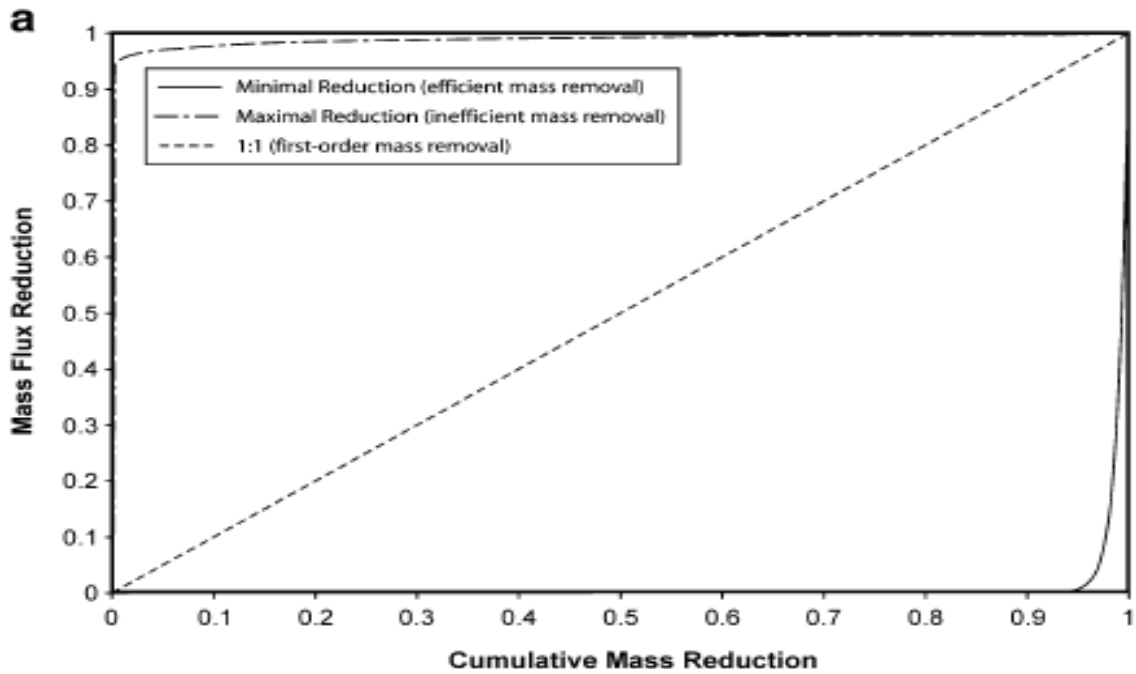


Figure 2. Mass flux reduction relationships from the dissolution of immiscible liquids in porous media; **a)** Theoretical relationships for mass flux reduction (from DiFilippo and Brusseau, 2008); and **b)** mass flux relationships calculated from a simple mass removal function.

Literature Review

Very little has been assessed as far as multi-component systems are concerned, which makes it all that much more important with regards to experimentation and scrutinization. However, heterogeneous systems have been investigated, but without consideration of the importance constant vs. changing interfacial surface area of NAPLs. Notwithstanding, laboratory experiments are paramount to the understanding of NAPL behavior. Only when variables are limited and isolated, then may they be fully comprehended.

Heterogeneity

Heterogeneity of a system can be characterized in multiple fashions. Two examples will be presented here. First, the subsurface itself can be considered heterogeneous. Thus, the composition of the media within an affected area varies from specific locations within that area. Various grain sizes and grain types may be present. Also, preferential flow paths may exist, which disturb flow within the strata. There may be differences in porosity and permeability. There can be a wide variety of multiple scenarios compounded on top of one another contributing to the complexity of a system. Very seldom is the subsurface considered homogeneous; however, these conditions are favorable during laboratory study as variables may be isolated in order to evaluate each facet of the overall system.

Secondly, there may be heterogeneity in the NAPL distribution. It is often propitious to present, or perceive, a NAPL to be in a single, solitary unit which directly infiltrates the subsurface. However, this is not often the case. NAPL distribution often infiltrates in “fingers” and permeates the subsurface along the paths of least resistance, and residing in the most favorable conditions. NAPL movement is resultant of the conditions in which it is subjected to. Thus, upon introduction to saturated zones, it tends to disperse and collect often. These

collections may be “pools” or “ganglia.” As a result, NAPL distribution pathways are often unpredictable (Pankow and Cherry, 1996). Consequently, it is misleading to perceive NAPL distribution as uniform, as this is seldom the case.

As convenient as it may be to utilize uniform media distribution in laboratory experiments, this is not often the case in real world applications. Complicated heterogeneity within the subsurface is commonplace. Complex interactions between heterogeneous media properties directly influence NAPL removal effectiveness. It has been shown that NAPL removal effectiveness varies spatially, as more constituent mass can be removed within receptive layers, but limited along boundaries of changing strata (Rao et al., 1997). Laboratory experiments have implemented ranging grain size distributions to simulate subsurface heterogeneity (Wright et al., 2010; Zhang et al., 2007) as well as field scale experiments conducted whereby the subsurface is painstakingly characterized with media ranging from gravels and unconsolidated sands to silts and clay lenses (Tick et al., 2003; Rao et al., 1997; McCray et al., 2011). While subsurface conditions are consistently varied by location, it has been exhausted that with increased heterogeneity, comes more unpredictable NAPL behavior. Highest rates of mass removal are found to occur in more hydraulically conductive zones, where the largest amounts of contaminant are located; however, long term residual contamination can occur in areas of lower hydraulic conductivity, even if these areas contain smaller amounts of mass (McCray et al., 2011). Less hydraulically conductive zones tend to be clay lenses or capillary barriers which often produce the presence of preferential flow paths. Preferential flow within an aquifer presents its own difficulties, as NAPL bypass flow does little with respect to NAPL dissolution behavior. Only when continuous contact of a solvent is observed can practical NAPL dissolution occur. The work of Zhang et al. (2007) exhibited this direct behavior of

preferential flow where the use of a 3-D flow cell allowed for the observation of source zone architecture on flow paths. Preferential flow took place in a coarse sand aquifer of the flow cell under saturated conditions. However, with the introduction of a NAPL, flow bypassed the coarse sand zone as the newly emplaced NAPL now occupied this zone. Thus, as heterogeneity continues to vary, resultant flow also varies.

NAPL Distribution

Not only does subsurface heterogeneity influence NAPL dissolution processes, but also the distribution of the NAPL itself can pose its own complications. According to Wright et al. (2010), it is the distribution of NAPL that determines the resultant mass transfer processes. Distribution of NAPL tends to be erratic and non-uniform (Anderson et al., 1992). Contaminant mass can exist in a variety of fashions. Laboratory experiments have determined that even under homogeneous conditions, NAPL infiltration occurs in “fingers” (Kueper and Frind, 1988). These “fingers,” once generated, induce the formation of others and disperse as a function of the heterogeneities of the media. The migration of these fingers can be unpredictable and extensive because they are subject to the environment in which the contamination occurs. Upon encountering a less hydraulically conductive zone, these fingers may become perched and result in pools. As long as there is sufficient NAPL present, pools may persist in favorable zones indefinitely. It has become evident that NAPL distribution plays a determining a NAPL saturation, as NAPL availability plays an ever more increasing role in apparent aqueous concentrations. NAPL distribution is directly related to subsurface heterogeneity; however, it is not expected to determine NAPL distribution.

Multi-component NAPL Ideality

Disposal of complex NAPL mixtures (gasoline, petroleum derivatives, and chlorinated

solvents) is commonplace at hazardous waste disposal sites (McCray and Dugan, 2002; McCray and Brusseau, 1998; Hinlein, 1999; Yu and Chou, 2000; Skubal et al., 2001). For this reason, it is essential for the study of the behavioral effects of one compound upon another. The understanding of the characteristics exhibited by a single-contaminant are not sufficient for the analysis of a multi-component NAPL, as the influence one compound has on the behavior of another complicates the complexity of the entire NAPL solution.

The single, most frequently detected organic contaminant found at hazardous waste disposal sites are the chlorinated aliphatic hydrocarbons (CAH; Broholm and Feenstra, 1995). These compounds are of extreme importance because of their proven toxicity, relatively high solubility, and resistance to biodegradation (OMB, 2011). Thus, these chlorinated compounds pose a serious health hazard even when present in small concentrations. It has been shown that minute mole fractions of CAH present is a general trend at military and industrial waste sites; these sites have typically noted mole fractions of CAH at or below 0.01 (McCray and Brusseau, 1998; Jawitz et al., 1998; Skubal et al., 2001). Even as these small mole fractions of CAH persist, chlorinated compounds (i.e. TCE) are still maintained as the primary contaminant of remediation interest.

Understanding multi-component NAPL dissolution behavior for equilibrium conditions is essential for adequate risk assessment (Brown et al., 1999). Predicted equilibrium conditions are often used in modeling and site characterization (Borden and Pivoni 1992; Seagren et al. 1999). Thus, order to conduct accurate assessments, the values used must also be accurate. A principal study was conducted by McCray and Dugan, 2002, which exemplifies this importance, as pre-existing acceptance of ideality of Raoult's Law was questioned. Various mole fractions of TCE: n-decane, ranging from 0.1 to 0.0001, were evaluated to assess the predictability of Raoult's Law

(Eq. 4). Batch experiments were conducted and column experiments were simulated with the various mole fractions to examine both static and dynamic conditions. Under static conditions, equilibrium was achieved with resulting gamma coefficients larger than unity (i.e. > 1), confirming the underestimation of Raoult's Law. Dynamic column experiments evaluated two scenarios of differing mole fractions (0.1 and 0.0001) while presuming a gamma coefficient 6.1. The results also confirmed non-ideal dissolution. Presumably, according to Raoult's Law, there should be a linear relationship between decreasing mole fraction and increasing gamma functions. Results indicated that values predicted from Raoult's Law greatly underestimated actual measured values. Thus, dissolution equilibrium behavior was clearly non-ideal. The degree of non-ideality of multi-component NAPLs is directly related to the dissimilarity of the components themselves (Lesage and Brown, 1994). When comparing an n-alkane and a chlorinated solvent, chemical structure and formula differences are can play a major role in non-ideality. It is important to note however, even as non-ideal dissolution may complicate predicting dissolution behavior, the measured concentrations often bypass Maximum Contaminant Levels and overall decline of concentrations occurs at a much faster rate.

CHAPTER 3: Rate Limited Diffusion and Dissolution of NAPLs in Groundwater

Introduction

Non-aqueous phase liquids (NAPL) are rate limited as only mass that is in direct contact with solvent (in this case water) can be dissolved. The purpose of this study was to evaluate the importance of constant vs. changing interfacial surface on dissolution behavior. By incorporating an insoluble component (i.e. hexadecane) it is possible to analyze a system with a constant interfacial surface area. Column experiments were conducted where elution curves and mass flux behavior could be evaluated for three scenarios: uniformly (homogeneous) distributed NAPL (TCE-U1), non-uniformly (heterogeneous) distributed NAPL (TCE-NU1), and a multi-component scenario containing both TCE and hexadecane (TH-U1). Static batch experiments (TCE-B1 and TH-B1) were also conducted in order to observe equilibrium conditions. Each scenario allows for individual variables to be isolated in order to observe its effects on diffusion and/or dissolution behavior.

Materials and Methods

Materials

Pertinent physical properties of both NAPLs, trichloroethene (TCE) and n-hexadecane (HEX), and utilized media can be found in Tables 1 and 2. Analytical grade TCE (>99.5% purity) was purchased from Sigma-Aldrich Chemical and n-hexadecane (>99% purity) was purchased from Alpha-Aesar. Column experiments were conducted using homogeneous 20/30-

mesh quartz Accusand® (Unimin Corp., Le Sueur, MN, USA) as the representative porous medium. Stainless steel columns were used (2.2 cm I.D., 7 cm length, Alltech Co.) in all of the experiments. The column was designed to have minimum void volume in the end plates and was fitted with 1-inch opti-flow endfittings. The sandy material has a porosity of 32%, and a bulk density of $1.78 \text{ g}\cdot\text{cm}^{-3}$, and an intrinsic permeability of $1.38 \times 10^{-10} \text{ cm}^2$. Particle densities and other properties of the sand are listed in Table 1. Twenty milliliter vials from VWR were used, along with Sun Sri crimp caps, during the static batch experiments. The flushing solution (i.e. nanopure water), porous media, glassware and vials, and stainless steel columns and parts were autoclaved (45-minute run cycle) prior to each experiment to prevent contamination and biodegradation.

Table 1. Properties of porous medium (20/30-mesh Accusand) for column experiments.

Property	Value
*Uniformity coefficient d_{60}/d_{10}	1.184 ± 0.039
*Mean grain size d_{50} mm	0.724 ± 0.031
Porosity	0.32
*Bulk density $\text{g}\cdot\text{cm}^{-3}$	1.78
*Organic carbon content	0.0003
*k intrinsic permeability cm^2	1.38E-10
*K hydraulic conductivity	1.29E-03

Note: * from Brusseau et al., 2002.

Table 2. Chemical properties of relevant compounds.

Compound	Molecular Weight, g/mol	Solubility mg/L	Density g/cm ³
Trichloroethene (TCE)	131.39	1,200	1.462
n-Hexadecane (HEX)	226.44	Insoluble	0.770

Multi-component Solution Preparation

The multi-component immiscible phase liquid was prepared as a 1:14 volume fraction (0.2: 0.8 mole fraction, TCE:HEX) trichloroethene and n-hexadecane mixture. The equation used to calculate mole fraction is as follows,

$$x_i = \frac{m_i}{\sum_{i=1}^k m_i} \quad \text{or, alternatively as} \quad x_i = \frac{m_i}{m_T} \quad (4)$$

Where, x_i is the mole fraction of component (i) of the NAPL mixture, k is the total number of components in the NAPL mixture, m_i are the moles of component (i) of the NAPL mixture, and m_T is the initial total moles of all organic components in the NAPL mixture.

Mixtures were prepared in 100 mL bulk volumes to aide in the in consistent use of homogeneous solutions throughout the duration of the experiment. Weights of the 100 mL vials (type A, borosilicate volumetric flasks) were taken before and after the addition of the HEX, minimizing head space, to evaluate the total volume of the 100 mL vial, which turned out to be 106.4 mL after correcting for density. Next, the volume fraction of TCE, 7.6 mL, was added and

subsequently placed on a Barnstead-Labline A-Class shaker table for a period of 5 days to ensure adequate homogenization. All experiments utilizing multi-component immiscible liquid solutions obtained samples in this method, discarding excess when the vials were opened as volatilization could compromise the volume/mole fraction accuracy. Specific mole fractions were chosen to ensure that the bulk of the mass would exist as the insoluble HEX liquid fraction. Thus, the volume of TCE would appear insignificant as the ratio of TCE mass reduction during dissolution would be minimized or negligible. Additionally, in order to maintain a constant NAPL-water interfacial area during the dissolution flushing experiments, it was essential to maintain the bulk of the multi-component NAPL volume as the insoluble HEX liquid fraction.

This method was chosen in order to achieve maximum constant surface area, given such large discrepancies between mole fractions. However, as this is the initial sample preparation mole fractions, this is not indicative of the actual moles present in the system. Thus, the subsequent equation was utilized to calculate the actual moles in the system based on the volume of NAPL injected and initially present in the column prior to the dissolution experiments. The equation (McCray and Dugan, 2002), is as follows:

$$m_T = \frac{V_N}{\sum_{i=1}^k \frac{x_i^N W_i}{\rho_i^N}} \quad (5)$$

where m_T is the initial total moles of all the components in the NAPL phase, V_N is the volume of injected NAPL, W_i is the molecular weight of component i , k is the total number of components in the NAPL mixture, and ρ_i^N is the liquid density of each component. By applying this calculation, it leads to a better assessment of the actual number of total moles in the system,

whereby a more accurate mole fraction of TCE: Hexadecane.

The above solution preparation was utilized in order to ensure that accurate mole fractions were incorporated throughout this study. However, as it is predicted that the more variant the mole fraction, the more non-ideal the behavior, a subsequent, more diverse, mole fraction was incorporated for an additional static batch experiment. A 1:1000 volume fraction (0.003: 0.997 mole fraction) TCE: Hexadecane solution was also prepared. Identical preparation methods were chosen with adjusted volumes (i.e. 0.1 mL TCE injected into 106.4 mL Hexadecane). Since such small volumes were used, it was chosen only to utilize this minute TCE designation for the more controllable static scenarios.

Dynamic Column Experiment

The first phase of the research focused on understanding the behavior of NAPL-water interfacial area on dissolution dynamics during aqueous water flushing conditions. Three different column systems were designed to test the effect of NAPL-water interfacial area on the dissolution process. Two of the column experiments utilized single-component TCE as the bulk NAPL phase distributed within the porous medium. These experiments were conducted to evaluate the effects of changing NAPL-water interfacial area on the dissolution process as the NAPL TCE mass and interfacial area is reduced. The third column experiment was designed to maintain a constant NAPL-water interfacial area throughout the dissolution flushing period. Since a small fraction of TCE (target contaminant) was mixed into an insoluble bulk n-hexadecane NAPL phase, the bulk NAPL is not expected to dissolve over the time scale of the

experiment. Therefore, the dissolution of TCE into the aqueous phase will have to occur at the bulk NAPL-water interface, which is expected to stay constant during flushing.

Autoclaved columns were incrementally filled and packed with Accusand (20/30-mesh size) to mimic subsurface conditions. The degree to which the column was packed depended on the condition to be tested. Two different packing techniques were implemented to produce a variation in packing structure and differences in NAPL distribution within the column system. The first column system was packed in a consistent approach to maintain uniformity in packing to ensure a more uniform distribution of NAPL in the column. Specifically, the column was filled with dry sand in 0.5 cm heights and packed with moderate pressure (using a dowel just less than the inner diameter of the column; 2.1-cm I.D.) and then subjected to light vibration (Fisher Scientific- Analog Mini Vortexer) for 3 seconds. This method was repeated for each 0.5 cm height until the column was completely packed with sand and the top endfitting was then secured. Both the top and bottom endfittings included a porous polyethylene screen (pore openings 0.2-mm) to keep the sand contained within the column ends. Conservative tracer tests (pentafluorobenzoic acid i.e. PFBA) conducted in the columns prepared in this manner yielded average Peclet numbers (Pe) of 82.7 (average) indicating advective dominant conditions with relatively consistent and uniform packing methods (Table 3). The second column system was packed in three bulk steps to produce a non-uniform packing within the column thereby resulting in a more non-uniform distribution of NAPL (i.e. pools or high residual saturated zones) in the column. First, approximately one-third (bottom portion) of the column length was filled with dry media (20/30 mesh Accusand) and packed lightly (using the dowel method); next, the second

one-third (middle) of the column was filled with sand above the first section and extreme pressure was applied by hand (using the dowel) in the packing process; and third, the top remaining third section of the column was filled with sand without applying any pressure during the packing process and capped with the top endfitting. Both the top and bottom endfittings included a porous polyethylene screen (pore openings 0.2-mm) to keep the sand contained within the column ends. Conservative tracer tests conducted in this column system produced Pe numbers around 12.7 (average), indicating more dispersion controlled transport due to more non-uniform packing (Table 3). For all column systems, the porous screen was selected for the systems to help ensure that trapping of NAPL did not occur between the frits and the endfitting during the imbibing of NAPL residual saturation establishment process.

Table 3. Peclet numbers resulting for various packed systems

Conservative Tracer Tests (PFBA)	Peclet # [Pe]
EXP-1_U (uniform pack)	82.8
EXP-2_U (uniform pack)	83.8
EXP-3_U (uniform pack)	81.6
AVG (uniform pack)	82.7
EXP-1_NU (non-uniform pack)	11
EXP-2_NU (non-uniform pack)	12
EXP-3_NU (non-uniform pack)	15
AVG (non-uniform pack)	12.7

Prior to the NAPL imbibing process, the columns were saturated with nanopure de-ionized (sterile) water for approximately 48-hours from the bottom up using a HPLC piston

pump (Lab Alliance, Acuflo Series I) to ensure stable displacement. The water saturation process was monitored by weighing the column over time and once the weight stabilized for over 12 hours (end of 48 hours), the saturation process was terminated and the columns were sealed. This saturation process allowed for the gravimetric quantification of the pore volume (volume of the voids) and porosity in each column system. These methods were consistent for the preparation of each of the column experiment (i.e. TCE:HEX uniform distribution, TCE uniform distribution, and TCE non-uniform distribution, or TH-U1, TCE-U1, TCE-NU1, respectively). Pore volumes and other NAPL conditions can be found in Table 4.

Table 4. Column experiment conditions for various systems

NAPL Scenario	Pore Volume (mL)	NAPL Injected (mL)	NAPL Retained (mL)	Residual Saturation, S_n (%)
TCE-Homogeneous	7.3	10	2.0	27
TCE-Pooled	11.3	10	3.4	30
TCE:Hexadecane	8.9	10	2.6	29

For the single component TCE experiments and the multi-component TCE:HEX experiment, the residual NAPL was established in the porous media packed columns utilizing similar methods described in Pennell et al. (1993), Bai et al. (1997) and Boving and Brusseau (2000). The NAPL (10 mL) was extracted into a gas-tight syringe placed horizontally upon a KD Scientific Model 780100 syringe pump. The location (i.e. top or bottom) of injection was dependent upon the density of the NAPL. For both of the single component DNAPL

experiments, TCE was injected from the bottom up. However, the multi-component LNAPL (1:14 volume fraction TCE:HEX) was injected from the top down as the bulk constituent (HEX) and the overall NAPL mixture (TCE and HEX) existed as LNAPL. The specific direction of NAPL injection were chosen to (i.e. upward for DNAPL and downward for LNAPL) to ensure stable displacement of the immiscible liquids relative to the residual water saturated porous media. Ten milliliters of NAPL was imbibed in all 3 cases of study (TH-U1, TCE-U1, TCE-NU1) at an injection rate of 0.2 mL/min (i.e. Darcy velocity = 0.05 cm·min⁻¹). The exact amount of injected NAPL was determined both gravimetrically and volumetrically by measuring the mass of the syringe before and after injection. NAPL displaced from the column was collected in a glass volumetric burette to calculate NAPL volume remaining in the column. Values and procedures for column experiment conditions are presented in Table 5.

Table 5. Experimental procedures for establishing NAPL and for dissolution flushing.

NAPL Scenario	Column Volume (cm³)	NAPL Injection Direction	Residual Flush Direction	Dissolution Flush Direction
TCE-Homogeneous	26.8	Bottom Up	Top Down	Bottom Up
TCE-Pooled	26.8	Bottom Up	Top Down	Bottom Up
TCE:Hexadecane	26.8	Top Down	Bottom Up	Top Down

Residual NAPL saturation conditions were then established by pumping aqueous nanopure water at aqueous saturation limit (i.e. solubility limit for TCE and TCE:HEX systems, respectively) for at a rate of 8.5 cm·hr⁻¹ for 2 pore volumes, followed by an additional 10 pore

volumes at a flow rate of $85 \text{ cm}\cdot\text{hr}^{-1}$. The direction of this flushing was also dependent upon the density of the NAPL. This direction of flushing was opposite of the NAPL injection (imbibing) direction (i.e. top down for the multi-component TCE:HEX system and bottom up for the single component TCE system). Each particular flow direction was chosen to ensure stable displacement conditions and to maximize the amount of mobile phase NAPL removed from the column. The free phase NAPL displaced from the column was collected in a glass volumetric burette and the amount of NAPL in the column was determined from the difference between the volume injected and the volume displaced from the column. Initial residual NAPL saturations are presented in Table 4. Once initial residual saturations were established, the aqueous phase dissolution flushing experiments were initiated and effluent TCE concentrations (aqueous phase) were monitored for the duration each of the three column experiments (i.e. TH-U1, TCE-U1, TCE-NU1).

The dissolution experiments were conducted under stable displacement conditions and therefore DNAPL (i.e. TCE) distributed systems were flushed vertically upward (bottom to top) and the LNAPL (i.e. TCE:HEX) system was flushed vertically downward (top to bottom). All dissolution experiments were conducted using nanopure sterile water at a flow rate of $0.18 \text{ mL}/\text{min}$ (i.e. $v_p = 8.7 \text{ cm}\cdot\text{hr}^{-1}$) to represent typical groundwater flow conditions. As mentioned previously, TCE elution curves were characterized by analyzing aqueous phase effluent TCE concentration over time. Samples were collected in duplicate throughout the duration of each experiment for analysis on UV-Vis spectrophotometer and gas chromatograph. Samples were collected until the instrument detection limits were reached, upon which the experiments were terminated. There was no observed immiscible liquid mobilization during any of experiments indicating that dissolution was the dominant mechanism of TCE mass removal. One set of

samples were analyzed for TCE concentration directly after sampling using the UV–Vis Spectrophotometer (Shimadzu UV-1700) at a wavelength of 207 nm. These samples were collected from the column using a glass syringe and the fluid was transferred directly to a 10-mL volumetric flask (diluted if necessary) and analyzed immediately on the UV-Vis spectrophotometer to minimize losses due to volatilization. The detection limit of this method was 0.1 mg/L. Schematic representation of experimental set-up used is illustrated in Figure 3. The duplicate samples for GC analysis were also collected using a glass syringe connected to the column effluent port. 5-mL of sample from the syringe were transferred (diluted if necessary) to a headspace vial and crimp sealed with Teflon septa and aluminum caps and immediately stored at 4 °C for analysis on the gas chromatograph (Shimadzu GC-17A), equipped with using the flame ionization detector (FID) and autosampler (AOC 5000, LEAP technologies). Method detection limits for these analyses were 0.01 mg/L. During the experiments, elution curves were obtained from the collected TCE concentrations over time until the detection limit (0.1 mg/L or 0.01 mg/L) of the analysis were reached depending on the instrument.

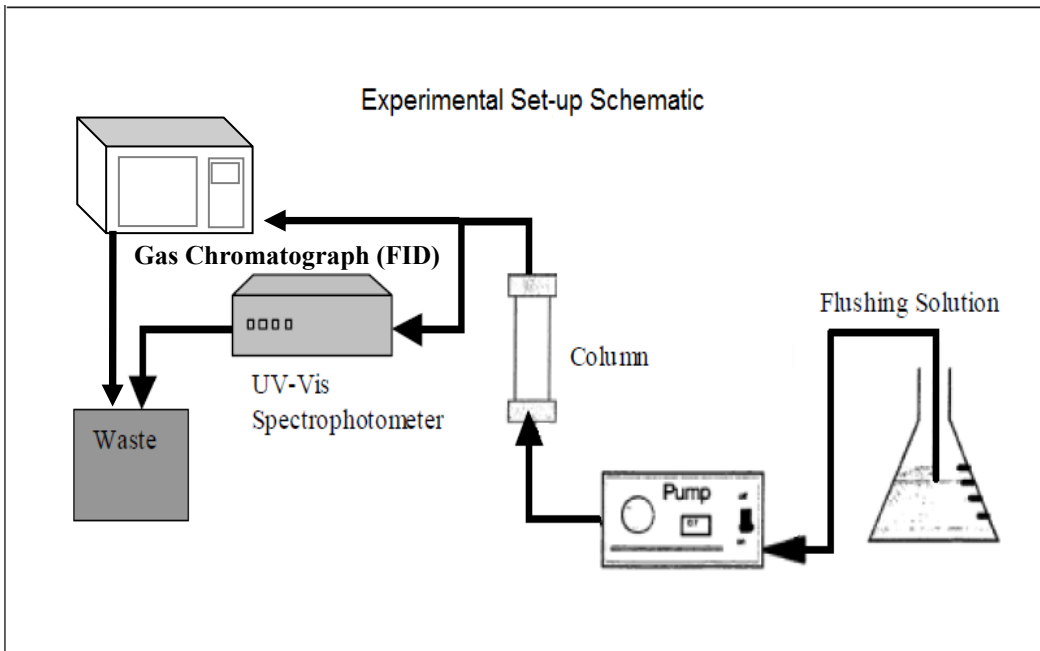


Figure 3: Schematic of Experimental Set-up.

Static Batch Experiment

The second set of experiments within the study assessed how the same contaminant set would behave under static, equilibrium conditions. A series of 20-mL headspace vials were arranged for a time series evaluation over a 48 hour period. Each series contained 10 vials to be tested at appropriate time intervals. NAPL preparation was identical to that in the dynamic scenario. A 10 mL NAPL sample, either single or multi-component, was placed in contact with 10 mL autoclaved nano-pure de-ionized water in a 20-mL vial, crimp sealed with Teflon septa and aluminum caps so that no head space was present. 10-mL bulb pipettes were used to replace the nano-pure water and 10 mL glass syringes were used for the NAPL emplacement. The fluid chosen (i.e. NAPL or water) to place in the vials initially was based on each fluid's density. Thus, for the single component experiments, TCE was placed first, followed by water.

Conversely, for the multi-component experiments (TCE + HEX), the LNAPL was placed on top of the water. This method was chosen in order to minimize NAPL mixing and agitation.

The first sample was taken after 30 minutes of NAPL-water interaction. Subsequent samples were taken in 90 minute increments for 11 hours. Two additional samples were taken after 24 and 48 hours to confirm that equilibrium conditions had been achieved. Samples were taken with a glass syringe from the aqueous phase analyzing the amount of dissolution and/or diffusion had taken place over that time period by measuring aqueous phase concentrations. Because of density differences between the single and multi-component NAPLs, sampling method differed. With the single component TCE batch experiment, aqueous TCE samples could be taken directly from the top of the vial, as the water is present above the TCE. Sampling aqueous TCE concentration from the multi-component (TCE:HEX) batch experiment required the use of a stainless steel hypodermic needle (10.2 cm) attached to the glass syringe. The needle allowed for the ability to acquire only sample from the aqueous phase, as the LNAPL pure phase was present above the water phase. Identical protocol was conducted during both studies with respect to sample analysis. Samples were analyzed for TCE concentration directly after sampling using the UV-Vis Spectrophotometer (Shimadzu UV-1700). Samples were collected from the vial using a glass syringe and the fluid was transferred directly to a 10-mL volumetric flask (diluted if necessary) and analyzed immediately on the UV-Vis spectrophotometer to minimize losses due to volatilization. Duplicate samples were also collected for analysis on the gas chromatograph. A 5-mL sample volume was extracted using a syringe and transferred to a 20-mL headspace vial, crimp sealed with Teflon septa aluminum caps, and then immediately stored at 4 °C until analyzed.

Results

Three distinct scenarios were tested over the duration of this study: a control containing the single contaminant, TCE, under ideal, homogenous conditions; a non-uniform NAPL distribution scenario under which TCE was injected into a “heterogeneous” (non-uniformly packed) porous medium condition; and finally a multi-component NAPL containing both TCE and n-hexadecane. Each system was prepared in the consistent fashion and executed with exact precision to ensure that the parameters being tested were, in fact, accurate and succinct. The samples collected for all experiments were done in duplicate; one set of samples analyzed using a gas chromatograph (FID detector) and one set of samples analyzed on a UV-vis spectrophotometer. This was conducted to confirm consistency between results and the experimental methods. The specific results for each experiment are presented and discussed in the following sections.

Dynamic Column Experiments

Single Contaminant - Uniformly Packed Conditions [TCE-U1]

This scenario is the most widely understood as it isolates a single contaminant under the most explicable conditions. Although this scenario is fairly rudimentary and has been previously conducted, it was performed here both for repeatability and comparison purposes. The aqueous solubility of TCE was selected as a mean value of 1,200 mg/L as it is comparable to previously reported values; 1100 mg/L (Pankow and Cherry, 1996), 1277 mg/L (Imhoff, 1992), 1421 mg/L (Broholm et al., 1992). Furthermore, three static immiscible liquid TCE-water phase systems were conducted to evaluate solubility of TCE for the conditions of the experiments herein. TCE aqueous solubility values also averaged 1,200 mg/L (Figure 10). It is widely accepted that aqueous solubility of TCE has been reported to be variable (somewhat of a moving target); thus a

mean value was chosen based on experimental determination and from observed literature values. Elution behavior was reported in three distinct phases: 1) Steady state phase at solubility, 2) Rapid decline in concentration due to dissolution, and 3) Tailing effects due to contaminant (TCE) mass depletion and significant reduction in TCE-NAPL surface area.

The initial steady state phase remained constant for a period of 102 pore volumes. This condition was corroborated on both instrumental analyses (GC and UV-vis Spec). Figure 4 presents measured over pore volumes flushed. Steady-state conditions result as the amount of TCE present is sufficient enough relative to the amount water flowing within the column to maintain maximum aqueous solubility and is controlled by the TCE-NAPL surface area is present. As water flows within the column the surface area of TCE decreases over time. Upon 102 pore volumes however, a critical point is achieved whereby surface area begins to decrease and aqueous concentrations also decreases. This decrease in concentration occurs over a period of 120 pore volumes. When the TCE-NAPL surface area has been significantly reduced to a critical point, and when most of the TCE mass has been removed, tailing occurs until the termination of the experiment at 360 pore volumes.

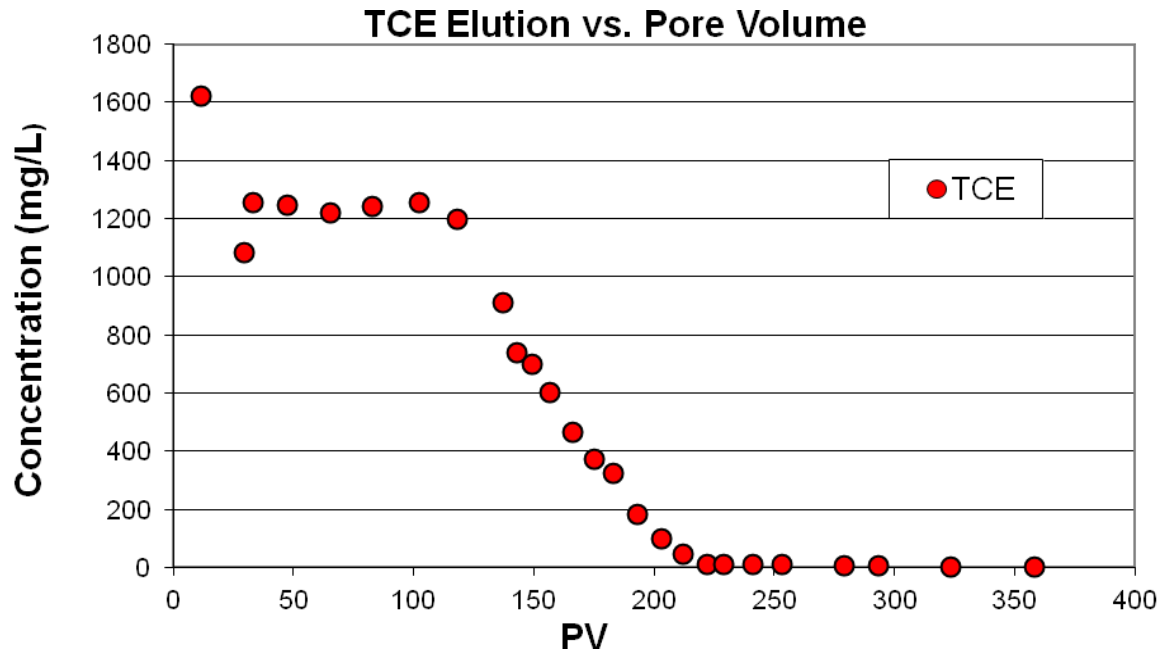


Figure 4: TCE elution curve [TCE-U1] under uniformly packed conditions. Data showing TCE concentration versus pore volumes of water flushed.

Mass flux reduction (MFR) behavior is plotted as mass flux reduction to fractional mass of TCE removed. Conditions for the uniformly packed experiment [TCE-U1] were optimum (maximum mass flux) until approximately 72% of the mass was removed from the column (Figure 5). This extended period of optimum MFR (maximum removal efficiency) coincides to the steady state phase and rapid dissolution phase observed in the elution curve (Figure 4). Optimal mass reduction occurs until a critical point is reached whereby there is an insufficient amount of NAPL surface area and mass present limiting the amount of interaction between the solvent (water) and the contaminant. The mass flux reduction behavior for this experiment [TCE-U1] demonstrated the greatest mass flux removal conditions of the systems tested as part of this research. As expected and shown in previous research, uniformly packed media (“homogeneous”) and uniformly distributed NAPL will lead to more efficient contaminant mass

removal. For example, maximum mass removal remained at a constant high rate for most of the duration of the experiment, followed by a drastic reduction of mass flux until most of the mass was removed from the column, at which time the experiment was terminated.

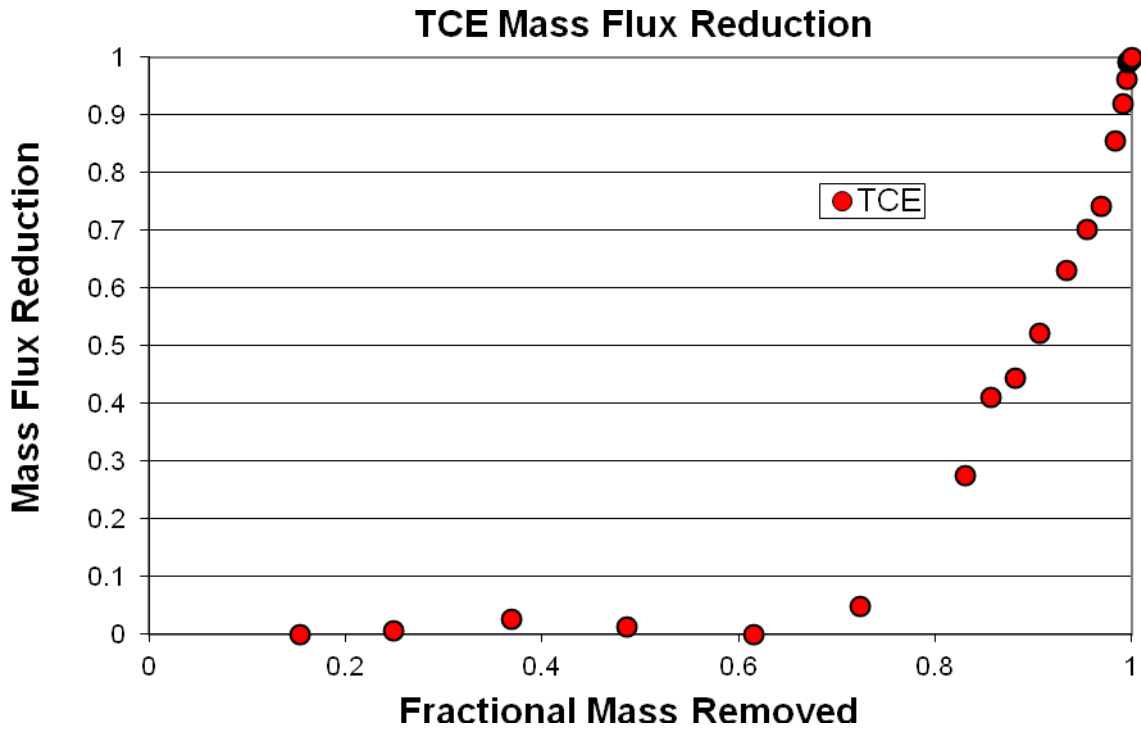


Figure 5. Mass flux reduction behavior under uniformly packed conditions [TCE-U1]. Mass flux reduction versus fractional mass removed.

Normalized TCE mass removal assesses the mass of TCE removed over time (i.e. pore volumes) with respect to total TCE mass removed. This initial case (TCE-U1) experienced mass removal at a rate of approximately 25% every 50 pore volumes (Figure 6). Upon 200 pore volumes flushed, 99% of the total TCE mass was removed from the column. This uniformly packed system (TCE-U1), resulting in a more uniform NAPL distribution through the column, produced quicker and more effective aqueous phase contaminant (TCE) removal as compared to

the non-uniformly packed system (TCE-NU1) with non-uniform NAPL (TCE) distribution. This more efficient removal process is likely due to the greater exposed NAPL interfacial area (more hydraulically accessible) associated with uniform residual NAPL saturations present within the system.

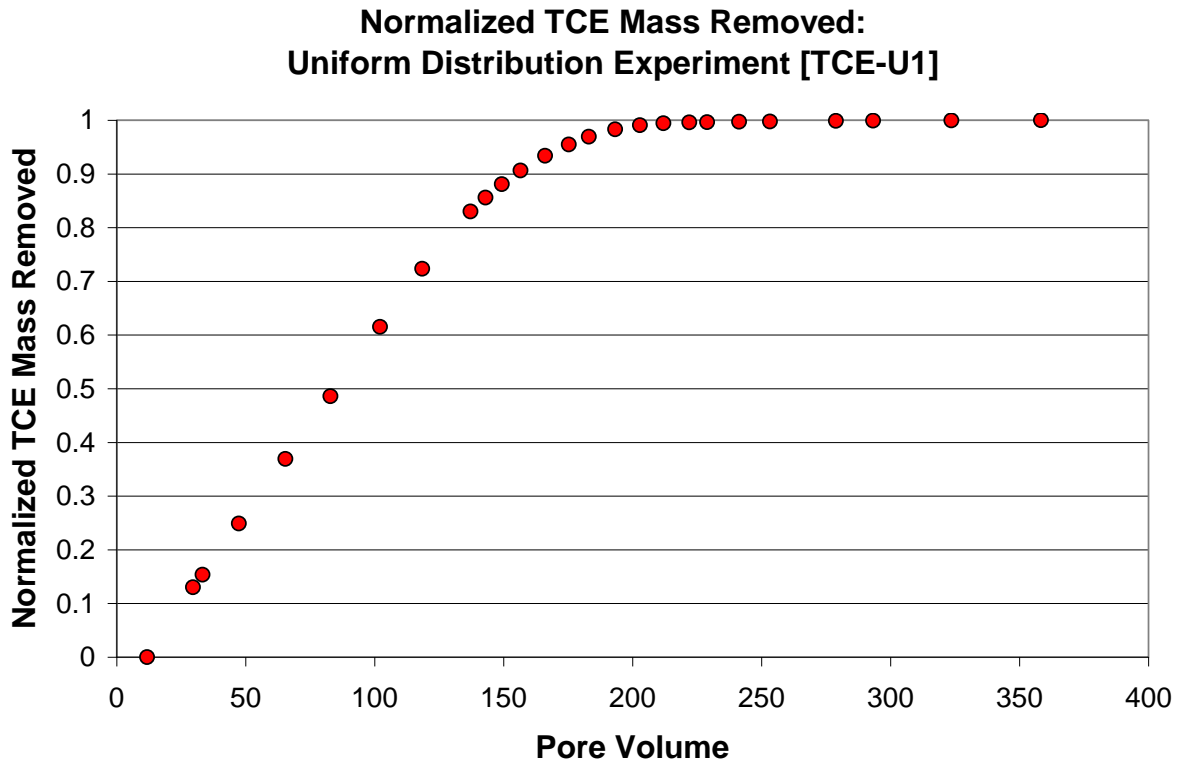


Figure 6. Normalized TCE Mass Removed for the Single-component TCE Uniform Distribution Column Experiment [TCE-U1].

Single Contaminant - Non-uniformly Packed Conditions [TCE-NU1]

Subsurface conditions at many contamination sites are known to be physically heterogeneous where the sediments exhibit significant variation in the particle size distribution. This “heterogeneity” can affect the distribution of immiscible liquids within the subsurface thereby controlling the rate of dissolution and contaminant mass removal during flushing (i.e.

pump and treat) conditions. Hence, a column NAPL-TCE dissolution experiment was conducted within a column created with non-uniform packing of the porous sandy medium. These conditions were created to test effects of non-uniform NAPL distribution and potential preferential flow paths on dissolution and mass removal processes. In addition, it is expected that varying NAPL saturations and even “pools” (or regions of high NAPL saturation) can form under these “heterogeneous” conditions. The presence of NAPL “pools” or regions of high NAPL saturation will limit the rates of dissolution due to the associated reduced NAPL interfacial area. NAPL “pools” or regions of high NAPL saturation can cause bypass flow or preferential flow around the NAPL, thereby limiting water-NAPL contact and resulting dissolution rates. This experimental scenario was implemented in order to assess the importance of changing interfacial surface area due to the presence of a non-uniformly distributed NAPL (i.e. TCE). Similar elution behavior as the uniform NAPL-TCE distribution experiment (TCE-U1) was observed, however, a “shouldering” effect with an additional steady state condition occurred (Figure 6). TCE elution was characterized in the following steps: 1) Steady-state elution (dissolution) at solubility (~1,200 mg/L) for approximately 170 PV, 2) Rapid concentration decline (~60 PV) as dissolution progressed, 3) Steady-state elution well below aqueous solubility (~300 mg/L) for 150 PV due to potential regions of NAPL “pools” or high saturation, 4) Additional rapid concentration decline (~50 PV), and 5) concentration tailing behavior for the remaining 200 PVs.

The initial steady-state phase remained constant for a period of 170 pore volumes. This steady-state phase is a bit longer than that of the uniformly packed column system (TCE-U1), but that is to be expected due to the fact that there was a higher initial residual saturation. Upon reaching 170 pore volumes, a rapid decrease in aqueous concentration occurred as a critical point

was met resulting in decreasing NAPL interfacial surface area of TCE. This decrease occurred over a period of approximately 60 pore volumes, until an intermediate steady state was reached. This “shoulder” in the graph is indicative of residual saturation having been exhausted with regions of “pooled” or high saturation NAPL still remaining, thereby contributing to the lower sustained steady-state elution phase. This steady-state phase in the elution curve persists for a period of 105 pore volumes at an aqueous concentration of approximately 300 mg/L. At a critical point (~ 335 PV), insufficient NAPL mass in the form of “pools” or high saturations and any remaining residual saturation occurs and TCE concentrations rapidly decline. This secondary rapid elution decline phase occurs until concentration tailing occurs at approximately 375 pore volumes. Tailing occurs throughout the duration of the experiment until termination at approximately 600 pore volumes.

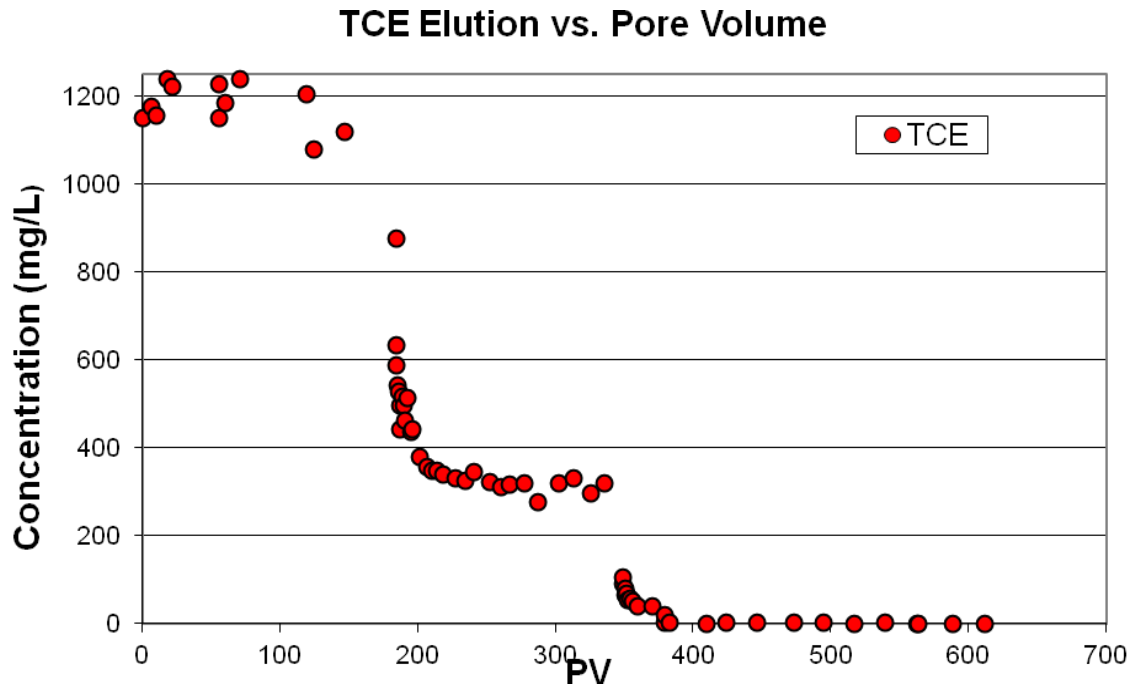


Figure 7. TCE elution [TCE-NU1] curve under non-uniformly packed conditions. Data showing TCE concentration versus pore volumes of water flushed.

Mass flux reduction (MFR) behavior is plotted as mass flux reduction to fractional mass of TCE removed. Conditions were similar to the uniformly packed column experiment (TCE-U1) as optimum mass removal (maximum mass flux) occurred until 72% of the TCE mass was removed. However, after a period of reduced mass flux, the “shoulder” is noticed as another “shoulder” is observed from 85% to 98% mass removal. The initial two steady state phases from the elution curve (Fig. 7) are coincidental with the steady state phases of the MFR graph (Fig. 8). This is also resultant of the dissolution reaching a critical point whereby sufficient surface area is limiting the amount of mass being removed; thus, mass flux is also reduced over these periods. The pooling of the NAPL is the basis of this limitation. As residual saturation is removed, mass removal is at its optimal level (i.e. highest MFR efficiency). However, as this depletion reaches

its critical point, pooled NAPL is subsequently encountered, at which steady state dissolution occurs, as it did during the initial phases of the experiment. Thus, this is evaluated as a function of decreasing interfacial surface area. The results of the MFR corroborate the results of the elution curve (Fig 8 and 7, respectively). Maximum dissolution results in maximum efficiency of mass removal. This occurs until a critical point is reached and mass flux is reduced. Upon encountering pooled NAPL, steady state conditions are once more achieved as MFR also stabilizes. Flushing continues and a subsequent critical point is achieved and MFR continues to rise until all the NAPL is removed.

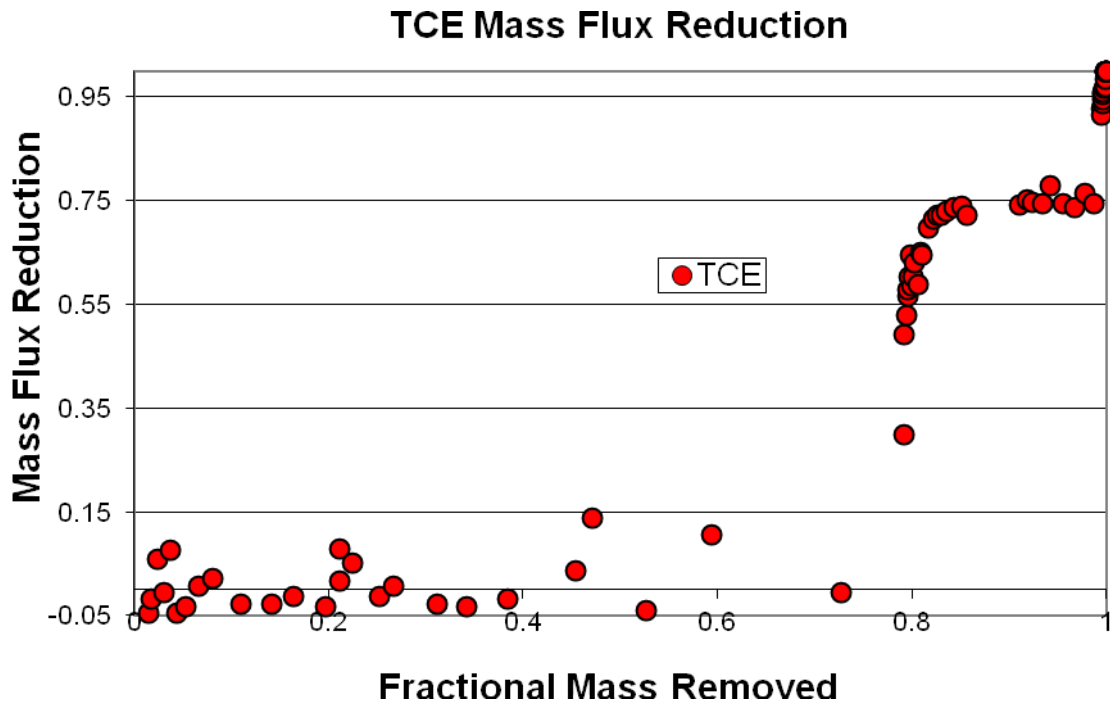


Figure 8. Mass flux reduction behavior under non-uniformly packed conditions [TCE-NU1]. Mass flux reduction versus fractional mass removed.

Normalized TCE mass removal assesses the mass of TCE removed over time (i.e. pore volumes) with respect to total TCE mass removed. The non-uniformly packed column system

with non-uniform NAPL (TCE) distribution (TCE-NU1) showed greater mass removal inefficiency compared to the uniformly distributed NAPL (TCE) experiment (TCE-U1) as would be expected. The —shoulder effects| observed on the TCE-NU1 elution curve (Figure 7) can also be observed on the normalized TCE removal plot (Figure 9). Constant (linear) mass removal is initially observed as a large fraction of TCE mass is removed from the column (~ 20% mass removal every 50 pore volumes). However, as dissolution continues and the majority of the accessible residual mass is removed (due to the higher available initial NAPL interfacial area), removal rates decrease likely as a function of remaining NAPL pools or zones of higher saturation and less hydraulically accessible NAPL mass as the reduced NAPL surface area of the remaining TCE in the system becomes a limiting factor for dissolution. Thus, at approximately 75% mass removal (180 pore volumes flushed) efficient linear dissolution trends decrease as the available NAPL surface area for dissolution is minimized. However, mass TCE mass removal continues until 99% of the mass is removed after 350 pore volumes flushed (Figure 9). This scenario showed the least efficient mass recovery in terms of normalized mass removal. The rate of dissolution was slower for this system compared to the other experiments (TCEU1 and TH-U1) requiring significantly more pore volumes of flushing to remove comparable amounts of TCE mass.

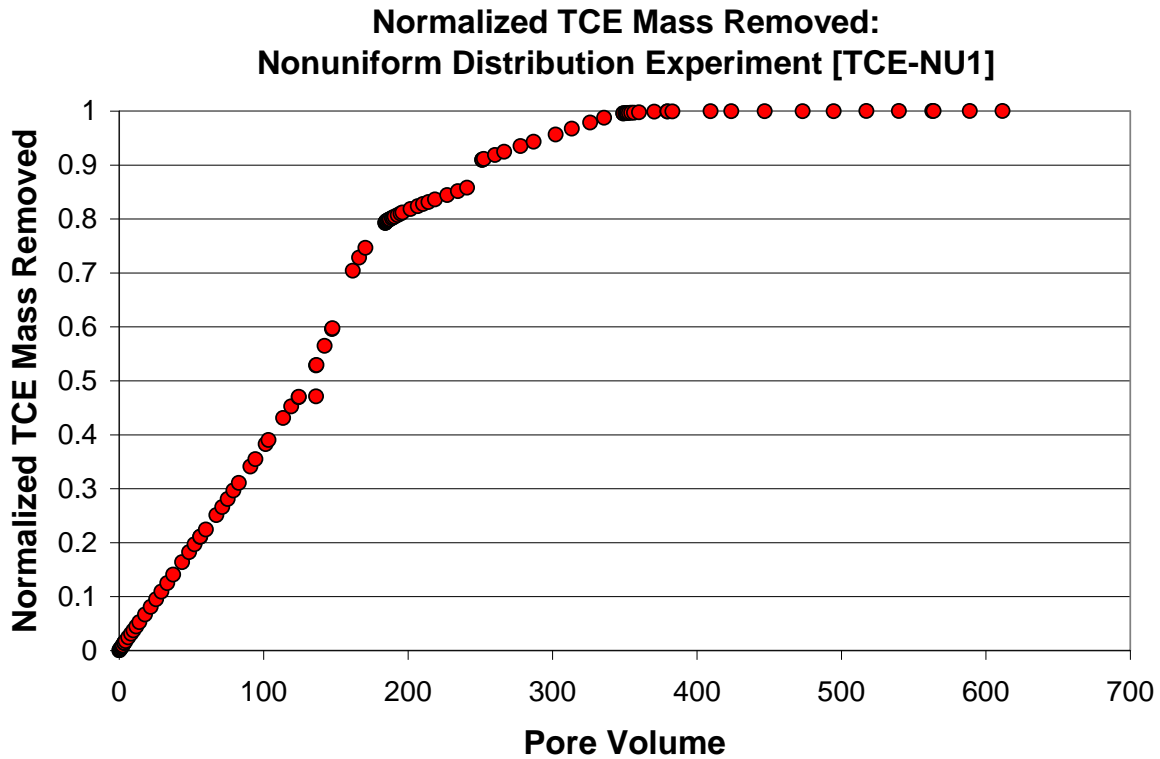


Figure 9. Normalized TCE Mass Removed for the Single-component TCE Non-uniform Distribution Column Experiment [TCE-NU1].

Multi-component Contaminant - Uniformly Packed Conditions (TCE:HEX) [TH-U1]

This experiment was conducted using a two-component NAPL mixture to evaluate the dissolution behavior of a target contaminant (TCE). The NAPL mixture consisted of a 1:14 volume fraction (0.2:0.8 mole fraction) of TCE to n-Hexadecane (HEX). The purpose of utilizing these two specific NAPLs was to understand the dissolution behavior of target contaminants within an insoluble bulk NAPL phase in which the bulk NAPL mixture does not undergo a change (i.e. decrease) in interfacial area during aqueous flushing. In other words, the bulk

NAPL-water interfacial area will remain constant during flushing as dissolution proceeds unlike single-component NAPL systems, where NAPL interfacial area decreases over time until complete removal. This was accomplished as HEX is considered insoluble over the time period of the dissolution experiment. By incorporating a 1:14 TCE:HEX volume fraction (0.2:0.8 mole-fraction) of a relatively more soluble compound (TCE) within an insoluble compound, the apparent NAPL surface area will remain essentially constant and therefore elution (dissolution) behavior will be independent of NAPL interfacial area reduction over time (i.e. during flushing). Elution behavior for this system differed significantly from the single-component dissolution experiments (TCE-U1 and TCE-NU1). Description of the general elution behavior for this system (TH-U1) is as follows: 1) brief steady-state TCE elution phase, 2) Relatively continual linear decrease in concentration (elution) without the presence of a concentration tailing phase. This indicates that the TCE dissolution rate is fairly constant during flushing and that intra-NAPL diffusion may be relatively constant during the time period of the experiment.

An extremely short period of steady-state elution was observed during the initial phase of this experiment (Figure 10). The steady-state elution phase lasted for approximately 1 pore volume and might be characterized by a negligible steady-state period in which the low initial mass and/or the rate of dissolution cannot maintain equilibrium concentrations. The rate of concentration decrease (i.e. related dissolution rate) during flushing is dramatically different than the previous single-component NAPL dissolution experiments (TCE-U1 and TCE-NU1). Concentration versus pore volume plots (elution curves) analyzed in log-linear scale shows that the concentration decrease over time is relatively constant, suggesting that dissolution rate is constant until aqueous concentrations can no longer be detected and, at which point, the experiment was terminated (Figure 10). Aqueous TCE concentration were exhausted at 0.02

mg/L without the presence of any apparent concentration tailing effects.

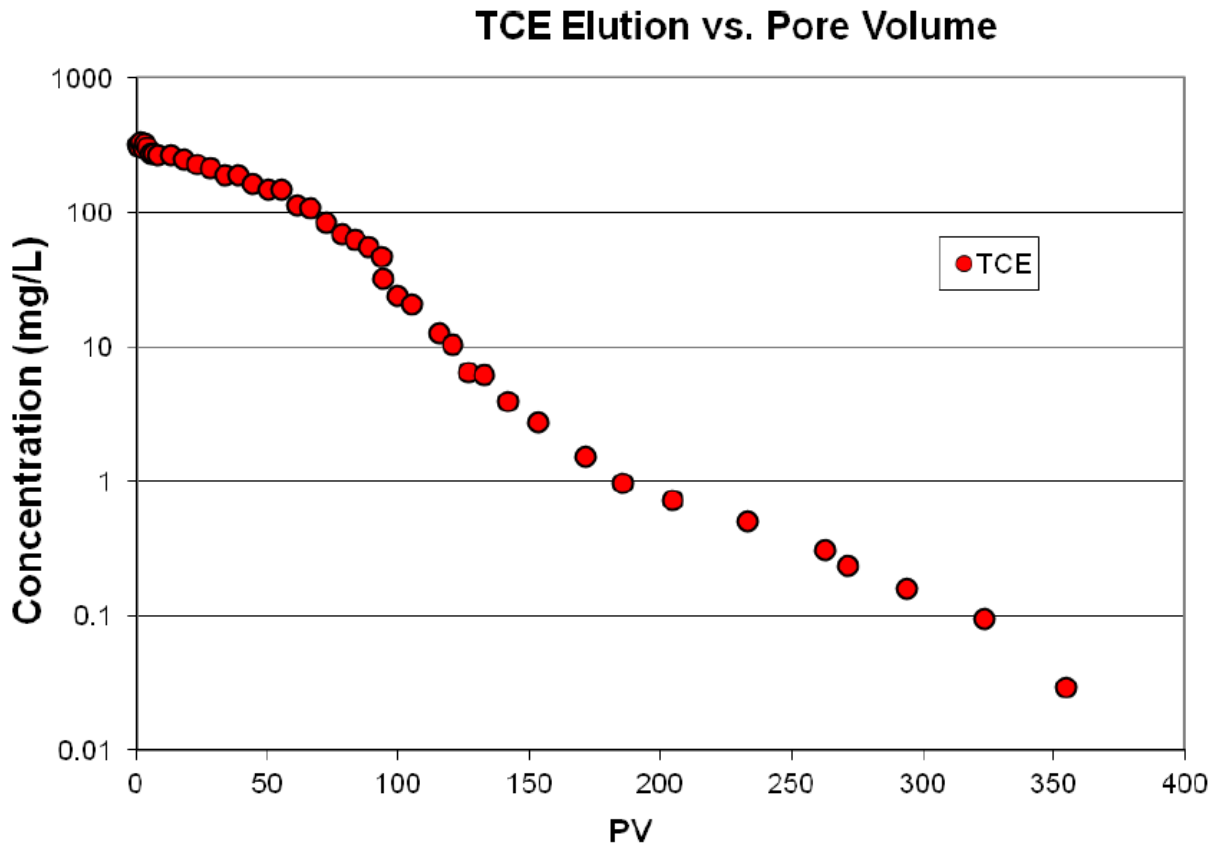


Figure 10. TCE elution curve under uniformly packed conditions for the two-component TCE:Hexadecane NAPL system. Elution data are presented in TCE concentration versus pore volumes of water flushed.

The observed mass flux reduction behavior (Figure 11) for this system was significantly different the two single-component TCE-NAPL experiments (TCE-U1 and TCE-NU1). The period of optimum mass removal efficiency (maximum mass flux) was relatively brief, occurring only during the first 30% of the mass removed. With still over 68% of the TCE mass remaining, the mass flux reduction begins increasing (mass flux decreases) indicating relatively nonideal mass removal conditions. At this point, a slow, steady increase in mass flux reduction continues

over the duration of the experiment until nearly all of the mass is removed. As mass flux was reduced by approximately 10%, the fractional mass removed from the column was also approximately 10%. This trend occurs until 80% of the mass was removed, at which point the mass flux reduction begins to increase at a slightly greater rate as only 5% of the TCE mass remains. However, the rate of mass flux reduction remains lower in this phase of the experiment (95% of the mass is removed) compared to the single-component TCE-NAPL experiments.

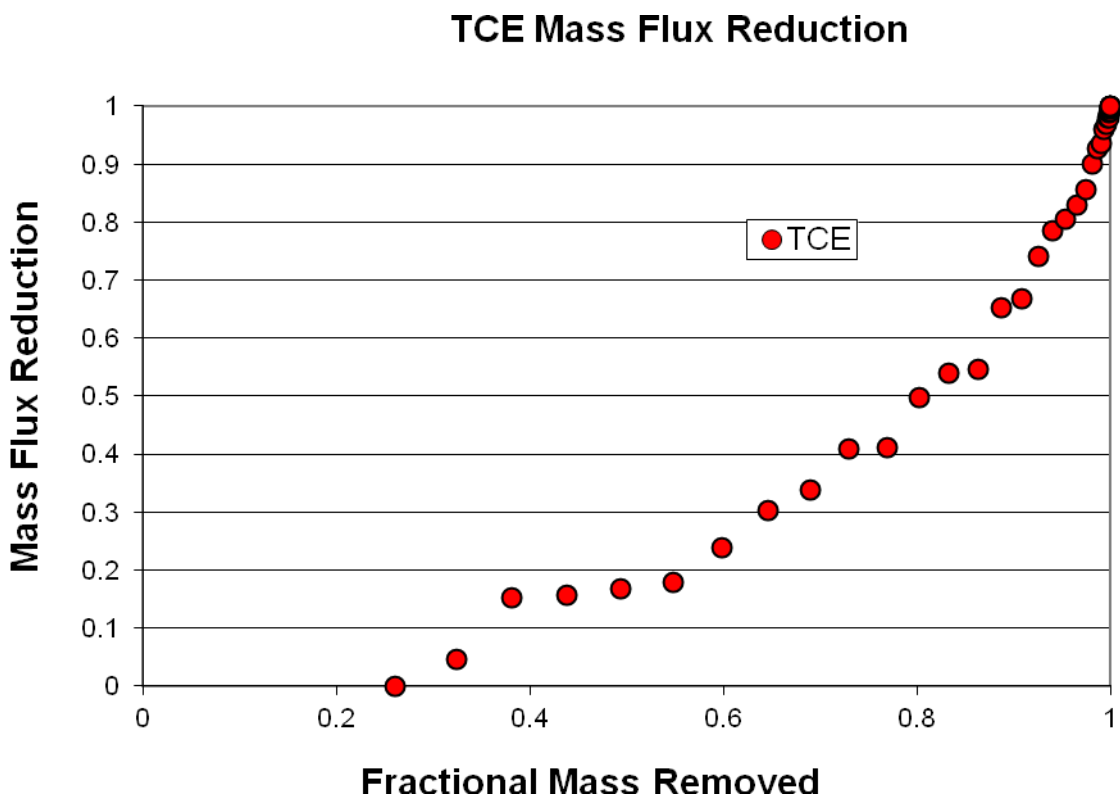


Figure 11. TCE mass flux reduction behavior under uniformly packed conditions for the two component TCE:Hexadecane NAPL system. Mass flux reduction versus fractional mass removed.

Normalized TCE mass removal for the multi-component (TCE:HEX) system (TH-U1) was the most efficient of all scenarios tested within this study. An observed constant rate of TCE dissolution during flushing (elution curve) resulted in more effective mass removal conditions (Figure 12). Approximately 65% of the TCE mass was removed from the column after 50 pore volumes of water flushing. It only took 125 pore volumes of flushing to remove 99% of total TCE mass from the column. The constant TCE removal suggests that the TCE within this multi-component NAPL system (TCE:HEX) is not experiencing significant intra-NAPL diffusion rate limitations. This indicates that there is sufficient TCE mass and a relatively constant rate of intra-NAPL (TCE) diffusion to the bulk NAPL boundary to maintain constant dissolution (elution) and mass removal behavior.

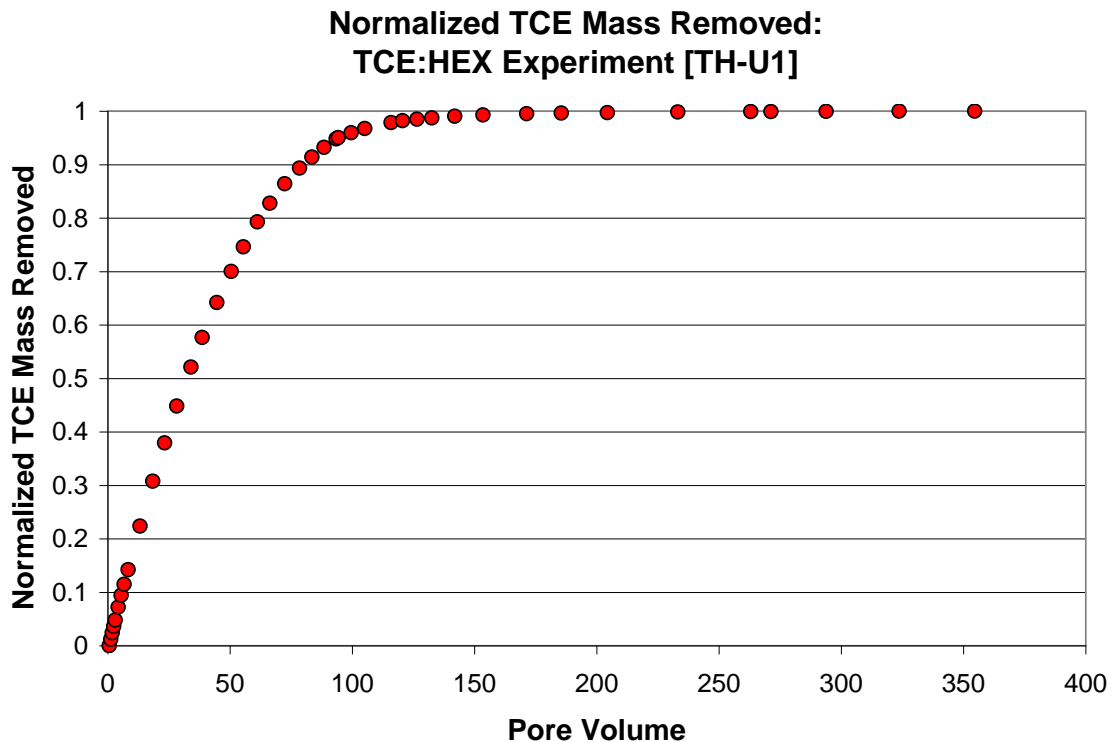


Fig 12. Normalized TCE Mass Removed for the TCE:HEX Column Experiment [TH-U1].

Equilibrium Batch Experiments

Single Component TCE

Ten milliliters of trichloroethene (TCE) were initially placed in the 20 mL glass vials followed by 10 mL of autoclaved, de-ionized nano-pure water. The vials were immediately crimp-sealed ensuring the system was completely sealed and devoid of headspace for any volatilization to occur. Two series of time-series batch experiments (TCE-B1 and TCE-B2) were allowed to sit and the aqueous phase TCE concentration was analyzed approximately every hour for 10 to 12 hours and then two remaining vials were sampled and analyzed at 24 and 48 hour time durations, respectively. Each vial was sacrificed after each sampling and analyzing event. Duplicates samples and analyses were executed for this experiment for repeatability purposes. The rate of dissolution (mass-transfer) was initially rapid. After the first hour of the experiment, aqueous TCE concentrations had already reached 489 mg/L. Aqueous TCE concentrations (dissolution) continued to increase at a rate of approximately $1.60\text{E-}05$ per second as TCE approached equilibrium concentration (average of two independent experiments, Figure 13). Both experiments reached solubility ($\sim 1,200\text{mg/L}$) after a period of 10 hours. As mentioned previously, additional samples were taken after 24 and 48 hours to ensure that equilibrium conditions had been achieved.

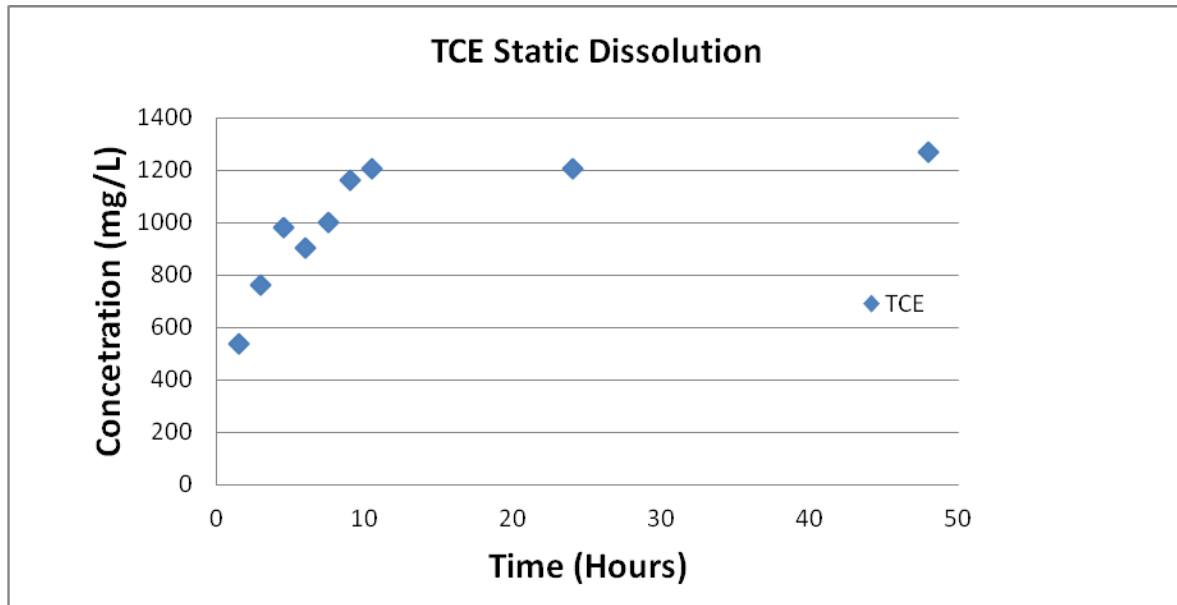


Figure 13. NAPL-TCE equilibrium time-series batch dissolution experiments (TCE-B1). Aqueous TCE concentration versus time.

Multi-component TCE:Hexadecane Equilibrium Batch Experiments

The TCE:HEX time-series batch experiments were conducted in a slightly different method due to the differences in density between the TCE:HEX NAPL mixture (i.e. LNAPL) and water. Ten milliliters of autoclaved, de-ionized nano-pure water was initially placed into 20 mL glass vials. This was followed by placing 10 mL of the 1:14 TCE:HEX volume fraction (i.e. 0.2: 0.8 mole fraction) LNAPL on top of the water already present in the vials. The vials were immediately crimp-sealed ensuring the system was completely sealed and devoid of headspace for any volatilization to occur. The collection of time-series TCE:HEX batch experiments (TH-B1 and TH-B2) were allowed to sit and the aqueous phase TCE concentration was analyzed approximately every hour for 10 to 12 hours and then two remaining vials were sampled and

analyzed at 72 and 120 hour time durations, respectively. Each vial was sacrificed after each sampling and analyzing event. Duplicates samples and analyses were executed for the experiments for repeatability purposes. Equilibrium aqueous TCE concentrations (i.e. nonideal dissolution) could not be predicted using a simple form of Raoult's Law where NAPL mixture activity coefficients γ_i^N are unity. Under this assumption, Raoult's Law predicted equilibrium TCE aqueous concentrations of 240 mg/L (0.2 TCE mole-fraction). The first sample analyzed (~30 minutes of water contact) produced an aqueous phase concentration of 64 mg/L. The time-series batch experiment (the remaining vials) continued (as dissolution occurred) until equilibrium TCE concentrations were reached at approximately 337 mg/L (Figure 14). Aqueous TCE concentrations increased at a linear rate of $1.4E-05$ per second for approximately 30 hours. Additional samples and analyses were taken at 72 and 120 hours to confirm equilibrium conditions.

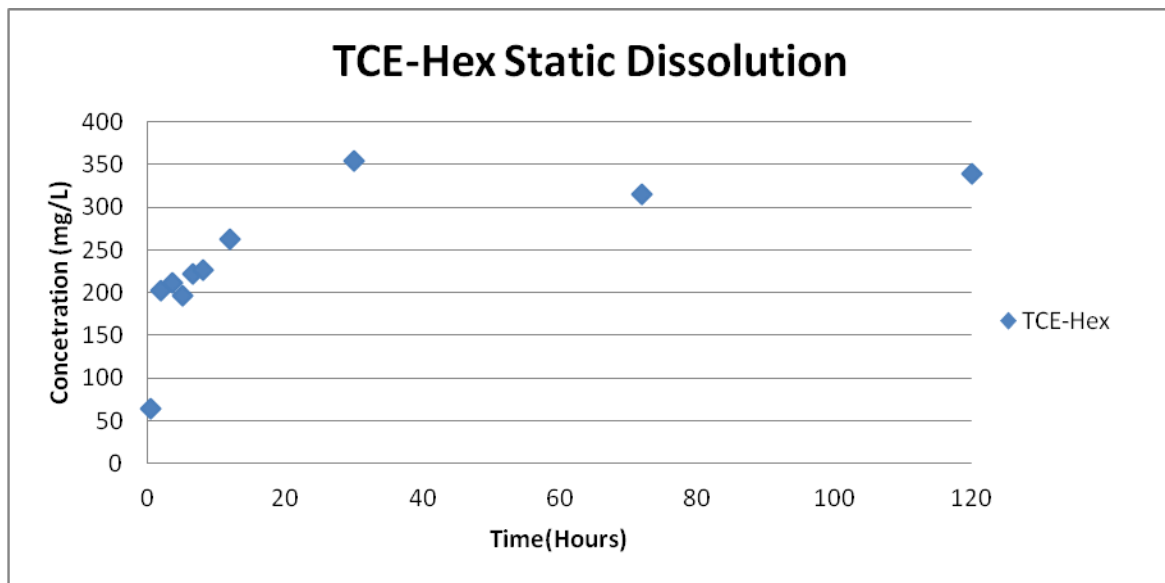


Figure 14. NAPL-TCE:Hexadecane (1:14 volume fraction; 0.2:0.8 mole fraction) equilibrium time-series batch dissolution experiments. (TH-B1). Aqueous TCE concentration versus time.

Considering that equilibrium aqueous TCE concentrations could not be predicted using a simple form of Raoult's Law where NAPL mixture activity coefficients γ_i^N are greater than unity due to nonideal dissolution for a 0.2:0.8 mole fraction, presumably activity coefficients (γ_i^N) would be larger for a more drastic mole fraction ratio (i.e. 0.003:0.997). Thus, it was decided to conduct a subsequent static batch experiment to evaluate the importance of smaller mole fractions of the constituents of multi-component solutions. Identical methodology was executed with respect to both mole fraction scenarios during sample preparation (see above method). Raoult's Law predicted equilibrium TCE aqueous concentrations of 3.6 mg/L (0.003 TCE mole-fraction). Interestingly, the first sample analyzed (~ 30 minutes of water contact) produced an aqueous phase concentration of 7.5 mg/L. The time-series batch experiment (the remaining vials) continued (as dissolution occurred) until equilibrium TCE concentrations were reached at approximately 25 mg/L (Figure 15). Aqueous TCE concentrations increased at a linear rate of $1.72\text{E-}05$ per second for approximately 11 hours. Additional samples and analyses were taken at 24 and 48 hours to confirm equilibrium conditions.

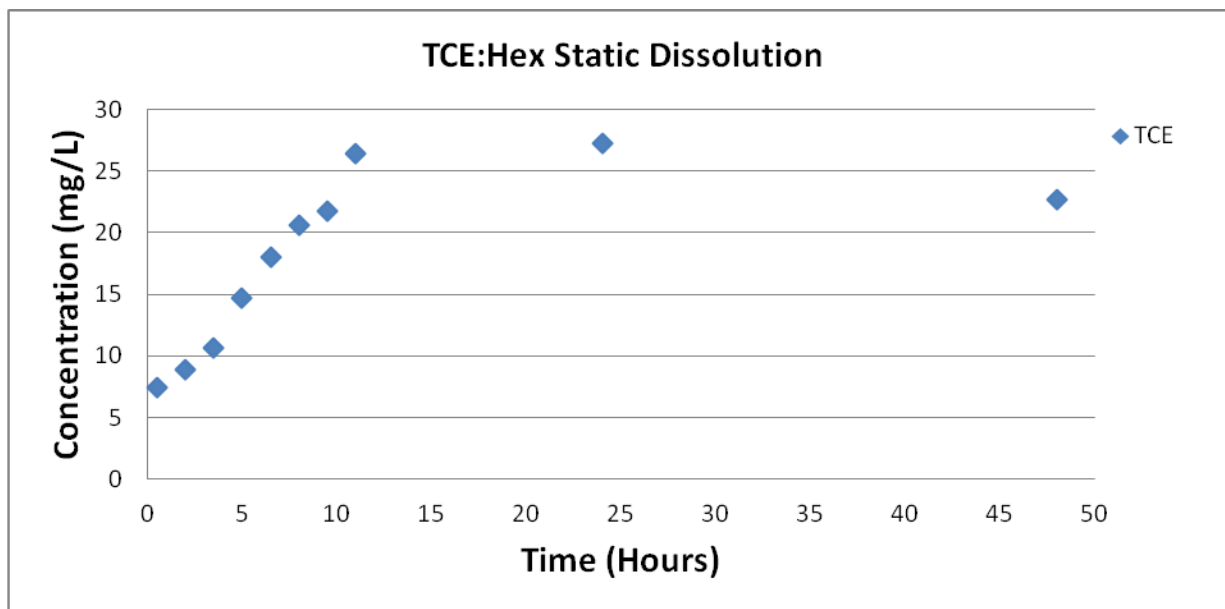


Figure 15. NAPL-TCE:Hexadecane (1:1000 volume fraction; 0.003:0.997 mole fraction equilibrium time-series batch dissolution experiments. (TH-B1). Aqueous TCE concentration versus time.

Discussion

Upon analysis of the multiple scenarios tested (TCE-U1; TCE-NU1; TH-U1), it is immediately evident that there are contributing factors controlling the response of TCE in aqueous and porous media systems. Each experiment was constructed in a way to understand how specific variables affect the dissolution of TCE from immiscible liquid (NAPL) sources. Each set of experiments are evaluated in terms of TCE elution response, mass flux behavior, mass removal efficiency, and equilibrium modeling (Raoult's Law prediction).

Single-Component TCE Dissolution Experiment: Uniformly Packed System

Conservative Tracer Tests

A series of initial experiments was conducted to ensure consistency in the packing methods of the porous medium (see procedure in Methods and Materials) and ensure advective flow for the systems. Confirmation of adequate column preparation was achieved by conducting conservative tracer tests using pentafluorobenzoic acid (PFBA) as the tracer of interest. A PFBA solution (250 mg/L) was pumped through the porous medium packed column at a flow rate of 0.18 cm³/min (linear $v_p = 8.7$ cm/hr) and continuously analyzed every minute using a flow through cell in a UV-Vis Spectrophotometer with a wavelength of 262 nm. The resulting breakthrough curves (data not shown) were modeled using CFITIM (Van Genuchten, 1981), a nonlinear least squares program, to determine swept pore volume, porosity, and Peclet (Pe) number. The results from the model were consistent with gravimetric measurements such as pore volume and porosity. The modeling results yielded relatively high **Pe** numbers (82.7 average) which indicated that transport mechanisms were predominantly advective and that the columns were packed in a consistent manner (uniform packed 20/30-mesh Accusand distribution). Once the initial porous medium packing conditions were confirmed to be consistent and producing advective flow conditions, the dissolution experiments could then be conducted.

TCE Dissolution Experiment [TCE-U1]

This experiment was conducted to evaluate the effects of changing NAPL (TCE) interfacial area on TCE dissolution and aqueous phase elution. As solvent (water) flows through the column there is a resulting change in NAPL-water surface area as TCE mass dissolves into the aqueous flushing solution. TCE removal and depletion rates are controlled (limited) by the reduction in NAPL-water interfacial area as mass is removed. Residually saturated NAPL

occupies a relatively small fraction of the pore space and remains as a stationary source of mass, as it is trapped within the pore spaces by capillary forces that cannot be overcome by typical hydraulic gradients. As water is pumped through the column, only a small fraction of the total TCE mass can dissolve into the aqueous phase (maximum 1,200 mg/L), dependent upon the specific aqueous solubility of the contaminant. Furthermore, under dynamic flow conditions where NAPL-water contact may be limited and where flow rates are greater than the NAPL mass-transfer rates (kinetically limited), aqueous effluent concentrations (TCE in this case) are expected to be significantly lower than solubility, especially after sufficient mass has been removed from the system. This phenomenon can be observed in TCE-U1; as water is pumped through the column, initial steady-state TCE conditions (maximum TCE aqueous solubility) are achieved as there is sufficient NAPL-TCE present to support these maximum concentrations for a period of time (Figure 4). However, as more solvent (water) is pumped through the column, NAPL-TCE mass and interfacial area are reduced whereby effluent elution TCE concentrations decrease at a relatively high rate until concentration tailing is observed. This reduction becomes noticeable on the elution curve once a critical point is reached as there is insufficient NAPL present to support solubility (equilibrium) conditions. Concentration tailing occurs when there is limited NAPL present (mass and interfacial area) in the systems and TCE concentrations decline at an extremely low rate. Contaminant mass flux is also limited when NAPL mass and interfacial area are significantly reduced. These conditions are directly observed near the end stages of the experiment (TCE-U1), as tailing and mass flux reduction behaviors are directly affected by reduction of NAPL surface area (Figure 5).

Single-Component TCE Dissolution Experiment: Non-uniformly Packed System

Conservative Tracer Tests

Physical heterogeneity within the subsurface is typical at many contamination sites throughout the world. For this reason, it is critical to design laboratory experiments that incorporate “heterogeneous” conditions in order to thoroughly understand dissolution dynamics and contaminant removal behavior in more complex systems. This “heterogeneous” scenario was tested by creating a non-uniformly packed porous medium system. Such non-uniformly packed sediment systems are expected to cause non-uniformly distributed NAPL consisting of NAPL “pools” or regions of high NAPL saturation. The purpose of this set of experiments was to evaluate NAPL dissolution and TCE elution due to both non-uniform NAPL source distribution and resulting induced preferential flow paths. It has been well documented that non-uniform NAPL distribution (i.e. “pools” and high saturation zones) can further limit the rates of dissolution due to lower exposed NAPL-water interfacial area associated with these systems.

A series of initial experiments was conducted to ensure consistency in the packing methods of the porous medium (see procedure in Methods and Materials) and ensure more dispersion-dominated flow regime (non-uniform packing condition). Confirmation of adequate column packing preparation was achieved by conducting conservative tracer tests using pentafluorobenzoic acid (PFBA) as the tracer of interest. A PFBA solution (250 mg/L) was pumped through the porous medium packed column at a flow rates and analyses were conducted in the same method as described previously. The resulting breakthrough curves (data not shown) were modeled using CFITIM. The results from the model were consistent with gravimetric measurements of pore volume and porosity. The modeling results yielded relatively low **Pe** numbers (12.7 average) which indicated that transport mechanisms were predominantly

dispersive and that the columns were packed in an inconsistent manner (non-uniform packed 20/30-mesh Accusand distribution). Once the initial porous medium packing conditions were confirmed to be non-uniform (“heterogeneous” packing) and producing dispersion dominant flow, the dissolution experiments could then be conducted.

TCE Dissolution Experiment [TCE-NU1]

The single-component TCE dissolution and elution behavior within the non-uniformly packed column (“heterogeneous”) systems exhibited significantly different behavior compared to the TCE dissolution experiment (TCE-U1) within the uniformly packed systems. Initially, both systems behaved similarly, exhibiting a steady-state TCE elution phase lasting approximately 120 pore volumes followed by a rapid decline in TCE concentration (transient dissolution phase) (Figures 4 and 7). The similarity of these behaviors results from the conditions under which the experiments were subjected and in which the initial period contains nearly the same hydraulically accessible NAPL mass and interfacial area. It is speculated that the initial rapid TCE concentration decline (after the initial steady-state period) occurs as the most hydraulically accessible TCE mass and interfacial area is depleted and/or where most of the NAPL is present as “pools/high saturations”. However, beyond this initial portion of the experiment, the elution behavior was drastically different. A secondary lower steady-state TCE elution (dissolution) and “shouldering” effect can be observed (Figure 7). A critical point occurs whereby sufficient NAPL and/or NAPL interfacial area exists to sustain this secondary steady-state elution phase. These concentrations could be sustained by the presence of numerous NAPL “pooled” or high saturation regions which contribute enough mass to maintain constant concentration conditions (i.e. ~300 mg/L) for an extended time period. As previously stated, NAPL dissolution is dependent upon mass-transfer between the NAPL interfacial area and bypassing water. As this

interaction occurs, NAPL “pools” or regions of high saturation are depleted and the resulting NAPL interfacial area is decreased to a point at which the TCE aqueous concentration cannot be maintained and a second rapid TCE elution decline is observed (Figure 7). A final extensive TCE concentration tailing phase is observed once most of the TCE mass is depleted and only a small fraction of the interfacial area exists to cause a very slow and steady decrease in aqueous phase concentration.

Multi-component (TCE:HEX) TCE Dissolution Experiment: Uniformly Packed System

Conservative Tracer Tests

A series of initial experiments was conducted to ensure consistency in the packing methods of the porous medium (see procedure in Methods and Materials) and ensure advective flow for the systems. Confirmation of adequate column preparation was achieved by conducting conservative tracer tests using pentafluorobenzoic acid (PFBA) as the tracer of interest. The exact same methods, described in the “Single-Component TCE Dissolution Experiment: Uniformly Packed System” (TCE-U1) section, were employed for this experiment to ensure uniform packing of the sediments in the column. The modeling results were the same as that discussed in the previous section, producing average **Pe** number of 82.7, which indicated that transport mechanisms were predominantly advective and that the columns were packed in a consistent manner (uniform packed 20/30-mesh Accusand distribution). The results from the model were consistent with gravimetric measurements such as pore volume and porosity. Once the initial porous medium packing conditions were confirmed to be consistent and producing advective flow conditions, the dissolution experiments could then be conducted.

TCE:HEX NAPL Dissolution Experiment [TH-U1]

Very seldom are there single components present at hazardous waste disposal sites, as various contaminants are often discarded or released together (McCray and Dugan, 2002; McCray and Brusseau, 1998). Hence, mixed contamination systems are ubiquitous and often occur as complex multi-component NAPL mixtures within the subsurface. Raoult's Law is commonly used to predict mass removal based on assumed mole fractions present through comparison of aqueous concentration elution and removal. However, if the NAPL mixtures consist of compounds that are highly dissimilar (i.e. molecular structure, composition, etc.), nonideality of dissolution behavior increases (Banerjee, 1984). Therefore, it is critical to understand the effects of dissolution nonideality on the removal of multi-component NAPL mixtures from soil and groundwater.

The TCE elution behavior and mass removal rates for the TCE-HEX experiment differed drastically when compared to the single-component TCE dissolution systems. An initial steady-state TCE concentration phase is essentially absent over the duration of the experiment. This indicates that there is not enough TCE mass dissolving into the aqueous phase to maintain such steady-state conditions. To some degree this is expected as the mole fraction of TCE within the NAPL mixture is relatively low (0.2). It is also possible that the intra-NAPL diffusion rate of TCE may be slower than mass flux of the system contributing to the immediate decline of TCE concentrations from the effluent (i.e. lack of steady-state phase) and inability to sustain constant TCE concentrations initially. As TCE dissolution proceeds during flushing, the aqueous TCE concentration (elution concentration data) continually and steadily decline over the entire duration of the experiment (Figure 8). In addition, there is no TCE concentration tailing phase as observed in the single-component TCE dissolution experiments. TCE concentrations of 1 mg/L

were reached in approximately 200 pore volumes compared to 350 pore volumes for the uniformly packed single-component TCE dissolution experiment (TCE-U1). Thus, in terms of evaluating mass removal based on concentration data, the continual TCE concentration reduction behavior of this system (TH-U1) seems to be a more favorable condition. Also, the multi-component system (TCE:HEX) is able to achieve lower aqueous TCE concentrations in less time due to a continual concentration decline without tailing effects. It is speculated that the TCE elution (dissolution) behavior observed in the multi-component NAPL (TCE:HEX) system is a result of the maintained constant bulk NAPL interfacial area (mostly n-hexadecane), in contrast to the decreasing interfacial area of the single-component TCE NAPL systems. Since n-hexadecane is insoluble, most of the NAPL volume and mass (TCE:HEX mole fraction 0.2:0.8) exists as hexadecane and the interfacial area will remain constant over the duration of flushing. As long as TCE intra-NAPL diffusion is relatively constant, the TCE exposed on the bulk NAPL surface area will experience relatively constant dissolution in the aqueous phase. Unlike single-component NAPLs, the constant NAPL surface area conditions of the TCE:HEX system allows TCE to constantly dissolve at a higher rate over longer period of time.

Initial aqueous phase TCE concentrations exiting the column were around 325 mg/L at which point immediate steady decline in concentration can be observed until the termination of the experiment (Figure 10). The ideal form of Raoult's Law under-predicted the observed effluent TCE concentrations, to be discussed in a subsequent section (Ideal and Nonideal Dissolution Modeling). A nonideality factor of 2.68, as incorporated through the NAPL phase activity coefficient (γ_{TCE}^N), was calibrated to model the aqueous phase TCE concentrations (Figure 22)

As each scenario was prepared in order to elucidate each variable's importance (i.e.

constant vs. changing interfacial surface, as well as varying mole fraction) on dissolution and mass removal behavior, comparison between each data set yields interesting behavior trends. Figure 16 compares dissolution behavior through the use of elution curves. The single component systems (TCE-U1 and TCE-NU1) experience steady state conditions, rapid dissolution, and tailing effects while the multi-component TCE:HEX (TH-U1) system behavior is constant removal without the presence of tailing.

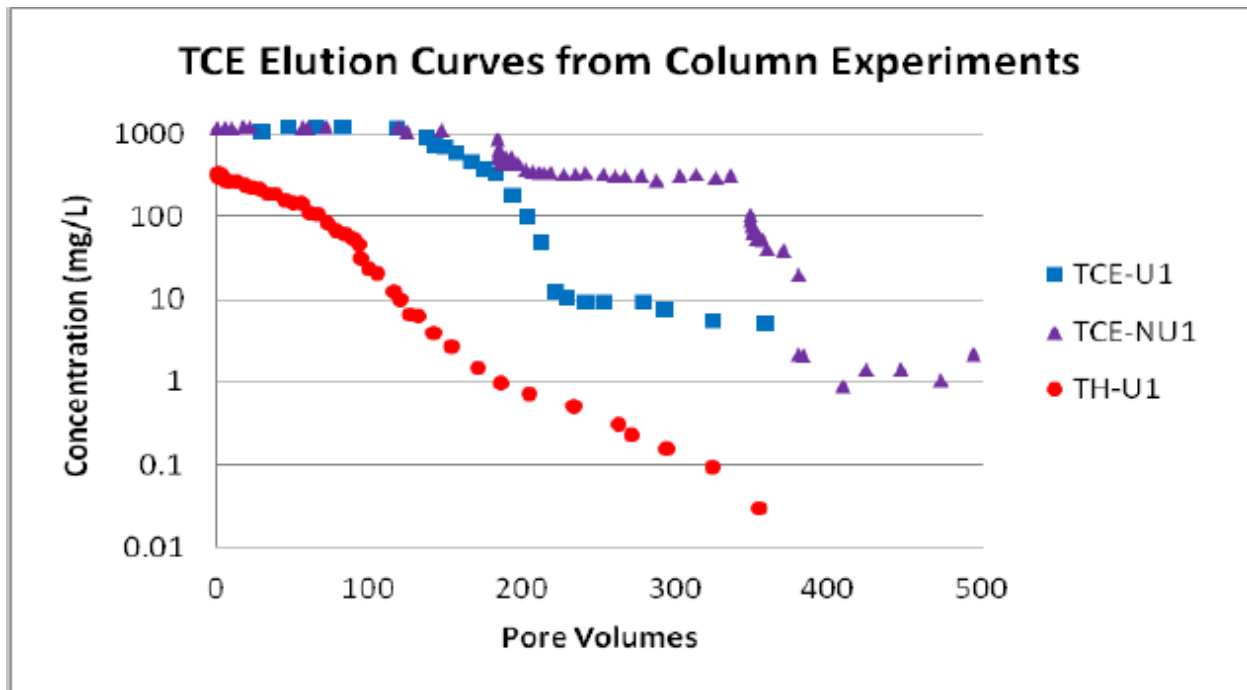


Figure 16. TCE elution curves from column experiments.

Mass flux reduction behavior differed throughout the duration of this study. The multi-component TCE:HEX (TH-U1) column study was the least efficient, as optimal mass removal was immediately reduced (Figure 17). This is most likely due to the small mole fraction of TCE present. Even as dissolution was constant (Figure 16), mass removal was inefficient. Both single component systems (TCE-U1 and TCE-NU1) had more favorable mass removal. TCE-U1 was the most efficient. TCE-NU1 encountered pooled NAPL and the “shoulder” condition

experienced (Figure 16) can also be observed in the MFR curve from 80-99% fractional mass removed.

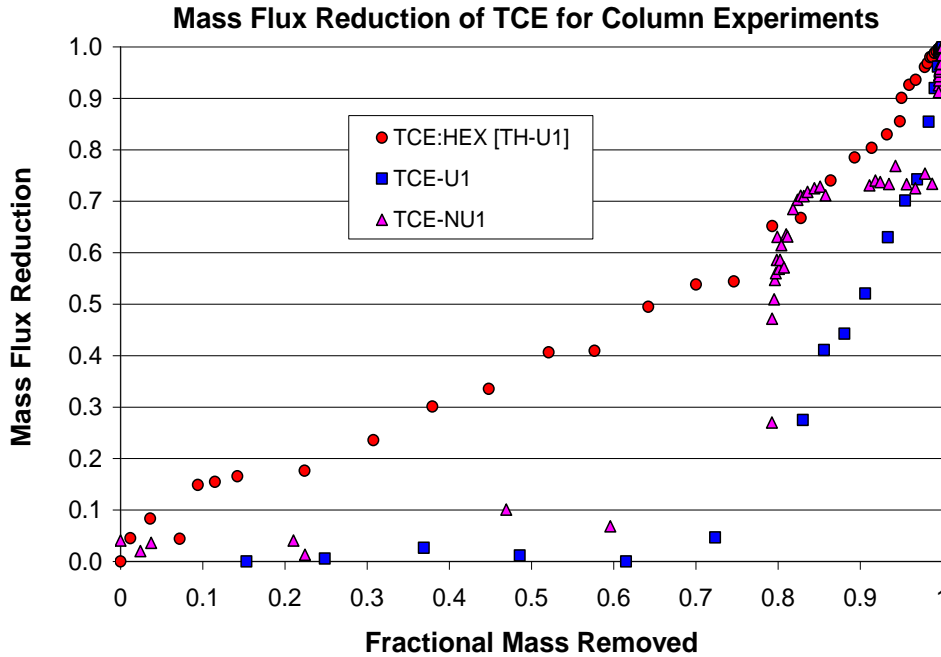


Figure 17. Mass flux reduction of TCE for Column experiments

Normalized TCE mass removal was comparable for all 3 scenarios tested within this study. TCE-U1 had median mass removal, which could be expected as this facet of the study was used as a control to reference the isolated variables to be tested (i.e. constant vs. changing interfacial surface area and varying mole fractions). TH-U1 resulted in the fastest normalized mass removal most likely due to the small mole fraction of TCE present (Figure 18). TCE-NU1 required the longest amount of time (most pore volumes flushed) to adequately remove TCE mass a surface area was limited due to the fact that NAPL distribution was non-uniform.

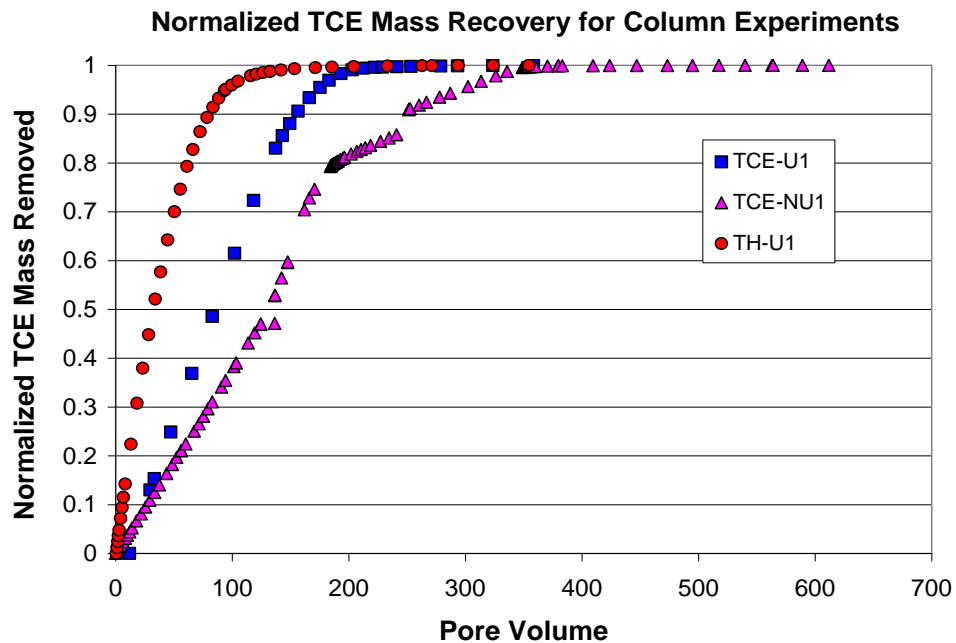


Figure 18. Normalized TCE mass recovery for column experiments

Time-series Batch Experiments

Single-component NAPL-TCE

The time-series batch experiments showed equilibrium results in which aqueous TCE concentrations increased with time until maximum concentrations were achieved (~ 1,200 mg/L) (Figure 13). A series of batch vials were prepared with NAPL-TCE and water at the same time and sampled approximately every hour to evaluate equilibrium dissolution. Each vial was sacrificed upon sampling and analysis. Aqueous TCE concentrations (average of duplicate samples) increased at a constant rate (i.e. $1.60\text{E-}05$ mg/L per second, Table 6) until concentrations stabilized at equilibrium values. Maximum TCE solubility was achieved after 10 hours at which point equilibrium conditions persisted (~1,200 mg/L). The results show that equilibrium conditions were achieved relatively quickly, given sufficient immiscible liquid

(NAPL-TCE) to support these high concentrations. Direct contact between NAPL-water interfacial area allowed for dissolution to occur over this relatively short time period.

Multi-component NAPL-TCE:Hexadecane- 0.2:0.8 mole fraction

The time-series batch experiments for the TCE:HEX NAPL system examined TCE dissolution from the NAPL mixture as a function of time. A series of batch vials were prepared with a 0.2:0.8 TCE:HEX mole fraction NAPL and water. Aqueous phase TCE concentrations were measured in the series of batch vials at the same time and sampled approximately every hour to evaluate equilibrium TCE dissolution. Each vial was sacrificed upon sampling and analysis. The bulk NAPL mixture was assumed to be uniformly distributed with TCE and the rate of TCE dissolution will depend upon the rate of intra-NAPL diffusion of TCE through the bulk NAPL to the NAPL surface area boundary. Aqueous TCE concentrations (average of duplicate samples) increased at a constant rate (i.e. $1.42\text{E-}05$ per second, Table 6) until concentrations stabilized at equilibrium values (Figure 14). Maximum TCE solubility was achieved after 30 hours at which point equilibrium conditions persisted. Dissolution was similar to the single-component TCE batch experiment, as aqueous concentrations increased at a linear rate until reaching maximum equilibrium concentration. However, the multi-component TCE:HEX NAPL (0.2:0.8 mole fraction) batch systems achieved notably higher aqueous concentrations than that predicted by the ideal form of Raoult's Law ($\gamma_{\text{TCE}}^{\text{N}} = 1$). Aqueous TCE concentrations reached equilibrium after 30 hours and maintained these conditions after 120 hours (337 mg/L-average) (Figure 14). Measured TCE equilibrium (maximum) concentration (i.e. 355 mg/L) was compared to predicted values from Raoult's Law to determine the degree of nonideality within the NAPL mixture. The nonideality factor can be expressed by the NAPL

phase activity coefficient ($\gamma_{\text{TCE}}^{\text{N}}$) which is equal to the measured TCE concentration (equilibrium) divided by the predicted concentration (i.e. ideal form of Raoult's Law). The NAPL phase activity coefficient ($\gamma_{\text{TCE}}^{\text{N}}$) was calculated to be 2.68, indicating a significant degree of nonideality and nonideal dissolution behavior. This nonideal behavior is likely due to the dissimilar molecular structure, compositional differences, and inherently low mole fraction of TCE within the TCE:HEX NAPL mixture discussed in previous sections.

Multi-component NAPL-TCE:Hexadecane- 0.003:0.997 mole fraction

The time-series batch experiments for the TCE:HEX NAPL system examined TCE dissolution from the NAPL mixture as a function of time. A subsequent series of batch vials were prepared with a 0.003: 0.997 TCE:HEX mole fraction NAPL and water. Dynamic mole fraction values are expected to increase the degree of nonideality in a multi-component system and the purpose of this facet of the study was to investigate this phenomenon. Aqueous phase TCE concentrations were measured in the series of batch vials at the same time and sampled approximately every hour to evaluate equilibrium TCE dissolution. Each vial was sacrificed upon sampling and analysis. The bulk NAPL mixture was assumed to be uniformly distributed with TCE and the rate of TCE dissolution will depend upon the rate of intra-NAPL diffusion of TCE through the bulk NAPL to the NAPL surface area boundary. Aqueous TCE concentrations (average of duplicate samples) increased at a constant rate (i.e. 1.72E-05 mg/L per second, Table 6) until concentrations stabilized at equilibrium values (Figure 15). Maximum TCE solubility was achieved after 11 hours at which point equilibrium conditions persisted. Dissolution was similar to the single-component TCE batch experiment, as aqueous concentrations increased at a linear rate until reaching maximum equilibrium concentration. However, the multi-component

TCE:HEX NAPL (0.003:0.997 mole fraction) batch systems achieved significantly higher aqueous concentrations than that predicted by the ideal form of Raoult's Law ($\gamma_{TCE}^N = 1$). Aqueous TCE concentrations reached equilibrium after 11 hours and maintained these conditions after 48 hours (22.3 mg/L-average) (Figure 15). Measured TCE equilibrium (maximum) concentration (i.e. 22.3 mg/L) was compared to predicted values from Raoult's Law to determine the degree of nonideality within the NAPL mixture. The nonideality factor can be expressed by the NAPL phase activity coefficient (γ_{TCE}^N) which is equal to the measured TCE concentration (equilibrium) divided by the predicted concentration (i.e. ideal form of Raoult's Law). The NAPL phase activity coefficient (γ_{TCE}^N) was calculated to be 6.1, indicating a significant degree of nonideality and nonideal dissolution behavior. This increased nonideality, with respect to the larger mole fraction (0.2: 0.8), confirms the assumption that disparate mole fractions influence the degree of nonideality within multi-component systems, as 0.2: 0.8 mole fraction solution resulted in a γ_{TCE}^N of 2.68 while the 0.003: 0.997 mole fraction solution achieved a γ_{TCE}^N of 6.1.

Table 6. Dissolution Rates for each Batch Equilibrium Condition

Solution	Mole Fraction	Trial 1 (1/ sec)	Trial 2 (1/sec)	Average (1/sec)	R ²
TCE	1	1.60E-05	1.60E-05	1.60E-05	0.89
TCE-Hex	0.2:0.8	1.78E-05	1.06E-05	1.42E-05	0.83
TCE-Hex	0.00:0.997	1.40E-05	2.03E-05	1.72E-05	0.98

Upon calculation of dissolution rates, it is evident that mole fraction is not a limiting factor controlling the rate of TCE dissolution. Each condition (i.e. mole fraction) was measured over time and rates of dissolution were calculated as each system achieved equilibrium. Values

were obtained with respect to maximum equilibrium solubility achieved (C/C_0) and plotted over time. All dissolution rates are similar, even with ranging mole fractions (0.003:0.997 to pure phase TCE). R^2 values were calculated revealing accurate linear trends of dissolution. The results of multi-component dissolution are indicative of constant intra-NAPL diffusion, as there seems to be sufficient NAPL mass (i.e. TCE) present at the NAPL-water interfacial to support constant dissolution rates. These results are interesting as regardless of the amount of NAPL mass present, the rate of dissolution into aqueous phase appears constant.

Ideal and Nonideal Dissolution Modeling

When comparing Raoult's Law (Eq. 1) to measured aqueous concentrations, it is immediately evident that the multi-component systems utilized within this study are nonideal. Mole fractions used to calculate predicted aqueous concentrations (i.e. 0.2:0.8 and 0.003:0.997) yield predicted initial aqueous phase concentrations of 240 mg/L and 3.6 mg/L respectively, using the ideal form of Raoult's Law (Eq. 1). The results of this study show that aqueous TCE concentrations from both static (batch) and dynamic (column) experiments do not reflect the values predicted by the ideal form of Raoult's Law. The source of mass-transfer nonideality can be attributed to the dissimilarity of the components within the NAPL mixture and the mole fraction dissolving into the aqueous water phase (Brahma and Harmon, 2003). The bulk NAPL in the investigated systems consisted of both 1:14 and 1:1000 volume fraction mixtures of trichloroethene: n-hexadecane (TCE:HEX), respectively. The NAPL of these proportions was chosen to maintain a constant NAPL-water surface area, as n-hexadecane (HEX) is considered insoluble. However, differences in molecular similarity, chemical structure, and chemical properties between the two chemicals were validated by the fact that nonideal partitioning

(dissolution) behavior was observed and represented by the two-component NAPL mixture system. n-Hexadecane is an n-alkane ($C_{16}H_{34}$) that is oriented in a chain/link structure (Figure 19). This molecular orientation is vastly different from that of TCE. TCE is a chlorinated aliphatic hydrocarbon (CAH) containing three chlorine atoms and one hydrogen atom bonded to double bonded carbon atoms (Figure 19). Both contaminants are organic compounds; however, dissimilarity in chemical structure and make-up create nonideal conditions when mixed as a multi-component NAPL solution.

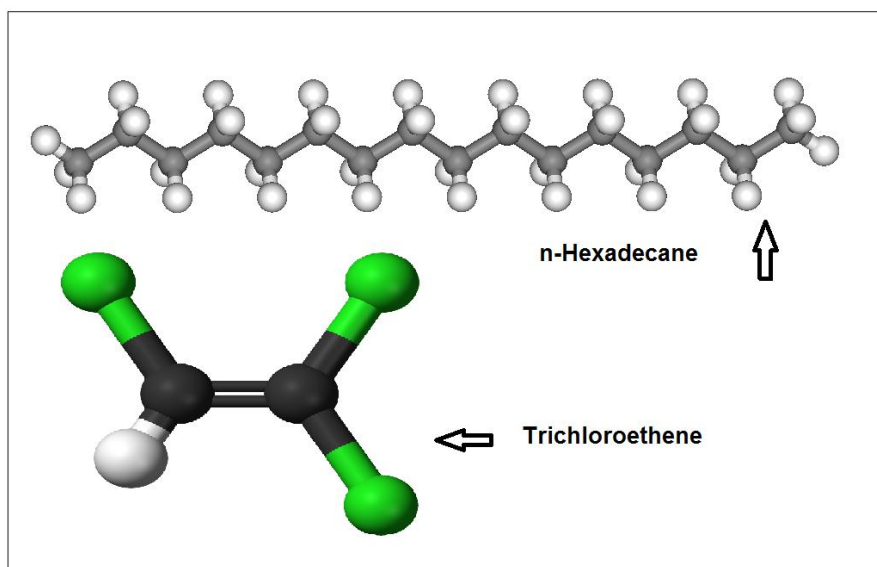


Figure 19. Three-dimensional representations of n-Hexadecane and Trichloroethene (TCE).

The measured TCE aqueous concentrations indicate the presence of nonideality in the system. Analyses of the chemical formulas and structures of each constituent give some indication behind the nonideality observed in the TCE-HEX experiments of this study. The batch and column experiments allowed to the determination of the degree of nonideality for static equilibrium conditions (i.e. batch experiments) and for potentially rate limited conditions

(i.e. dynamic column experiments). Evaluation of measured and predicted values allowed for an insight into this nonideal dissolution as a result of complex chemical mixtures (i.e. TCE:HEX NAPL mixture). Equation 4 can be used to calculate the total initial moles present in the NAPL mixture injected into the porous medium packed column. The injected NAPL volume (TCE and HEX) was 2.6 mL which consisted of a 0.2:0.8 TCE:HEX mole fraction (Table 7). As mentioned previously (Methods and Materials section), a larger initial mole fraction was used for the multi-component column experiments compared to the time-series batch experiments. This mole fraction ratio was chosen to reduce errors associated with NAPL-mixture preparation and injection into the column system. Extremely minute mole fraction (i.e. ≤ 0.01) NAPL mixture injections using milliliter volume syringes can introduce significant error in mole fractions if small deviations (\pm) during preparation or during injection occur. Since the TCE:HEX NAPL mole fraction (0.2:0.8) is dominantly hexadecane by volume, the bulk NAPL interfacial area will remain constant over the duration of aqueous flushing (i.e. dissolution).

Table 7. Multi-component NAPL (TCE:HEX) column experiment conditions.

TCE:HEX Column Experiment Conditions	
<i>Initial NAPL Conditions – Volume/Gravimetric</i>	
Total NAPL Mixture Volume [mL]	2.6
Volume of TCE in Mixture [mL]	0.18
Volume of HEX in Mixture [mL]	2.42
TCE:HEX Mole Fraction	0.2:0.8
*Total Moles (m_T) [$mol/TCE + mol/HEX$]	0.01
Moles of TCE	0.002
Moles of HEX	0.008
Volume Fraction TCE:HEX	1:14
<i>#Initial NAPL Conditions – Moment Analysis</i>	
Total NAPL Mixture Volume [mL]	2.58
Volume of TCE in Mixture [mL]	0.19
Volume of HEX in Mixture [mL]	2.39
TCE:HEX Mole Fraction	0.21:0.79
*Total Moles (m_T) [$mol/TCE + mol/HEX$]	0.01
Moles of TCE	0.002
Moles of HEX	0.008
Volume Fraction TCE:HEX	1:14

*Calculated by equation (4)

#Assumed that most of the TCE mass was removed during flushing

The TCE:HEX column dissolution experiment (TH-U1) was terminated upon reaching method detection limits of the instrumentation analysis. It was assumed that nearly all of the TCE mass was removed over the time period of aqueous flushing. Moment analysis and total TCE mass removed allowed for the calculation of initial TCE mass in the NAPL mixture. Thus, conditions such as initial moles, initial total moles of the mixture, and initial mole fraction for TCE and n-hexadecane (as the NAPL mixture) could be determined (Table 7). Since 0.002 moles

of TCE was recovered from the moment analysis of measured values, the appropriate mole fraction of TCE in the NAPL phase was 0.21 (Eq. 5). By applying this mole fraction to Raoult's Law (Eq. 1), the predicted value TCE was 252 mg/L. However, initial values exiting the column were reported as 321.2 mg/L. Figure 20 illustrates the differences between measured and predicted TCE concentrations. Each predicted concentration value differs proportionally relative to decreasing mole fractions. It is evident that the ideal equilibrium predicted elution curve under predicts the actual TCE concentration elution profile. This suggests that mixture nonideality plays a significant role on dissolution, resulting elution behavior, and mass removal for complex NAPL mixture systems. In this case, the nonideality effect would contribute to greater contaminant mass removal than that predicted by ideal dissolution (Raoult's Law).

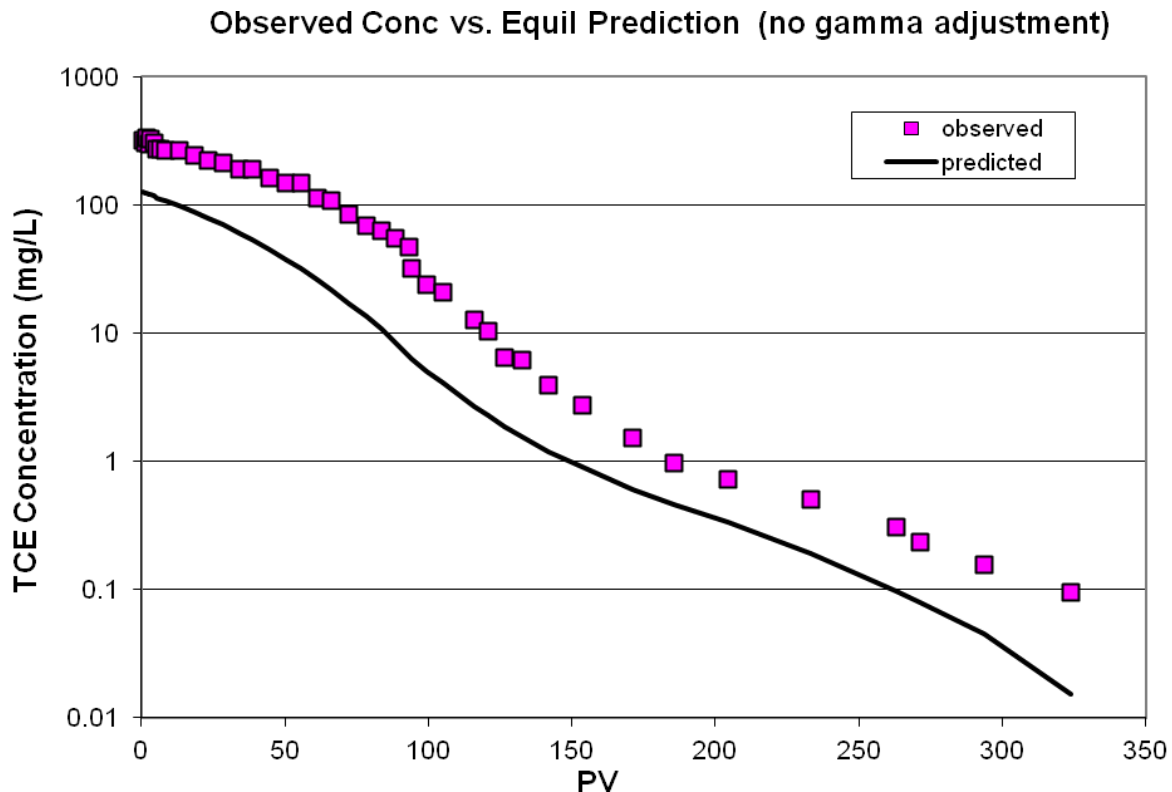


Figure 20. Multi-component TCE: Hexadecane. Observed TCE concentration vs. predicted TCE concentration from ideal form of Raoult's Law [activity coefficient ($\gamma_{TCE}^N = 1$)].

The inconsistency between predicted and measured concentrations can be accounted for by incorporating nonideality through the activity coefficient of the particular component within the NAPL mixture (γ_i^N) as determined by the following expression (eq. 6);

$$\gamma_{TCE}^N = \frac{C_{TCE}^W(\text{measured})}{C_{TCE}^W(\text{ideal})} \quad (6)$$

where the ratio of the measured concentrations divided by the predicted (ideal) concentrations provides a NAPL activity coefficient for describing nonideal dissolution. γ_{TCE}^N was calculated for each time step (moment analysis) based on the decreasing mole fraction as TCE dissolution and aqueous phase elution progressed. As mole fraction changed during flushing, resulting predicted TCE concentrations also changed. Figure 21 depicts the change of TCE mole fraction in relation to amount of pore volumes flushed through the column.

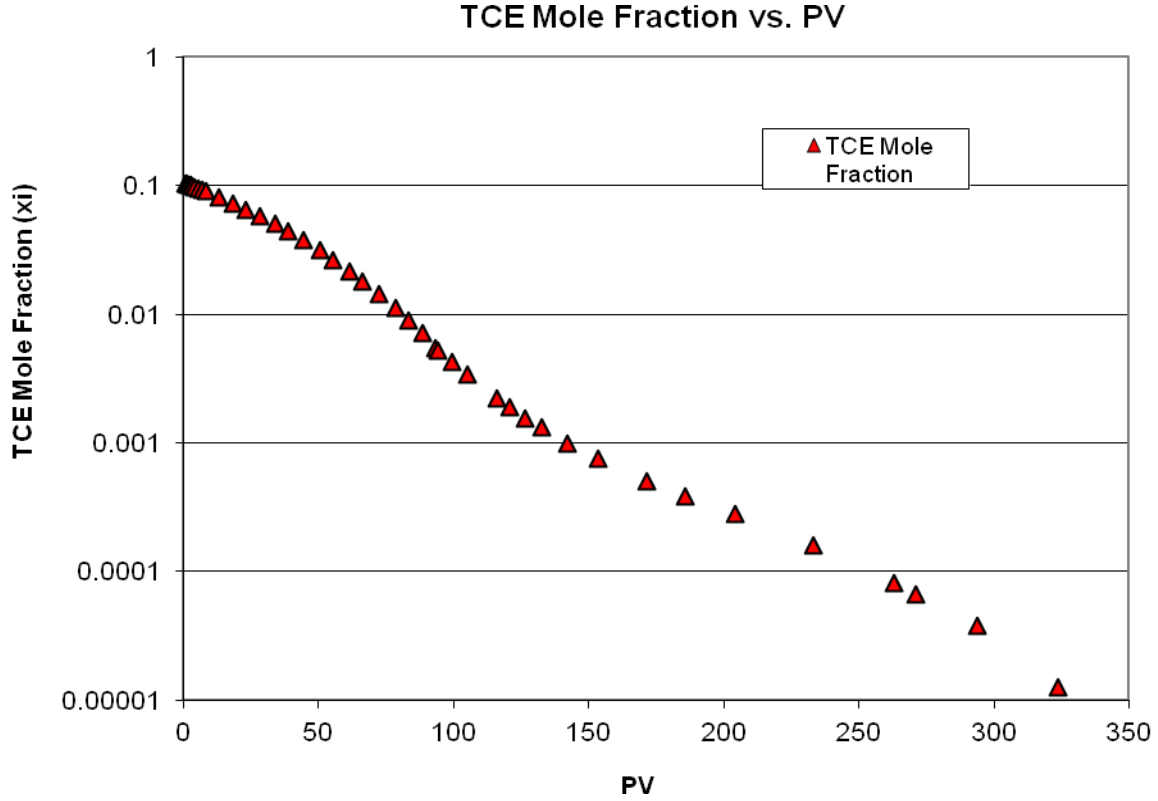


Figure 21. Multi-component TCE:Hexadecane dissolution experiment [TH-U1]. TCE mole fraction (x_i) versus pore volumes flushed.

In order to account for nonideal dissolution effects, a TCE predicted elution curve was modeled to fit the observed TCE elution concentration curve. This modeling analysis was conducted by generating a best-fit curve through activity coefficient ($\gamma_{\text{TCE}}^{\text{N}}$) calibration. The $\gamma_{\text{TCE}}^{\text{N}}$ was calibrated by minimizing the root mean square error (RMSE) between observed and simulated TCE concentrations. The RMSE function is as follows;

$$\text{RMSE} = \sqrt{\frac{\sum (C_{\text{sim}} - C_{\text{obs}})^2}{N}} \quad (7)$$

where C_{sim} is the simulated concentration incorporating the calibrated γ_{TCE}^N , C_{obs} is the measured concentration, and N is the number of observations. As mentioned above, the calibration process was continuously repeated until the best-fit γ_{TCE}^N returned the smallest RMSE between observed and predicted TCE concentrations. In general, the modeled curve provides a good match to the observed concentration data and overall trend (Figure 22). It should be noted that certain portions of the modeled curve slightly over-predict or under-predict observed aqueous TCE concentrations. This may be attributed to the variability and or error in sampling (i.e. dilution factors) or may be related to rate limited NAPL dissolution or mass-transfer/residence time effects due to the flow rate conditions of the experiment. Mass transfer limitations (kinetic controls on dissolution) could also result from NAPL bypass flow and preferential flow conditions within the column system. If aqueous phase concentrations vary slightly from sampling method, mole fractions would also be correspondingly affected. If mass-transfer rates are lower than effective flux, it is expected that the model would over-predict observed concentrations eluting from the system.

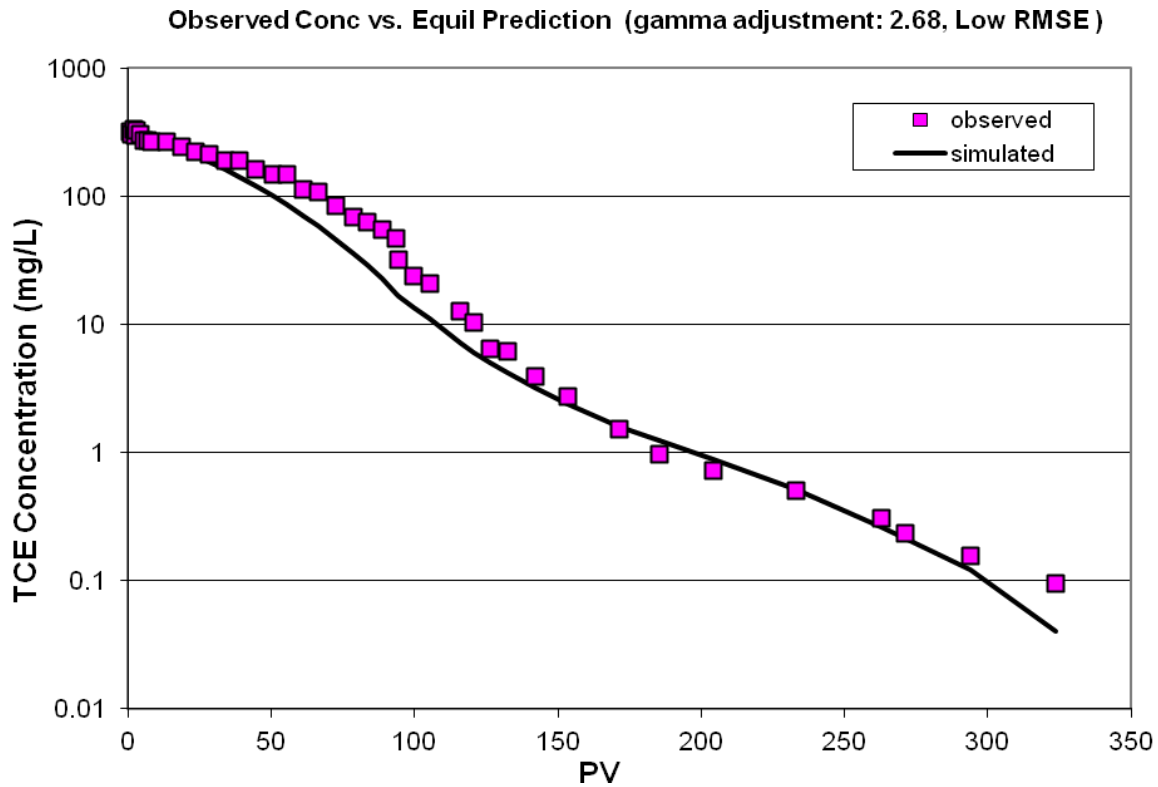


Figure 22. Multi-component TCE:Hexadecane dissolution experiment [TH-U1]. Observed and simulated TCE concentrations versus pore volumes flushed.

With comparative data between both dynamic (column) and static (batch) experiments, γ values can be more accurately predicted. Differences in equilibrium behavior and potentially rate limited behavior can be evaluated by examining these separate systems. The time-series batch experiments evaluate the time it takes to reach maximum equilibrium concentrations for a system in which the aqueous phase is static. The column systems examine (kinetic controlled) effects on dissolution rates and elution behavior during continual flushing with “clean” water. Kinetic-controlled rate limitations during dissolution can limit aqueous phase concentrations from reaching equilibrium conditions. However, static batch conditions allow for equilibrium concentration to be achieved during dissolution process given enough time. As a result, it is

expected that static batch conditions may result in higher relative aqueous concentrations than that observed in dynamic flushing experiments. To make appropriate comparisons, the NAPL mixture systems must be characterized based on mole fractions. Mole fraction of the NAPL mixture will be the primary factor controlling aqueous phase dissolution or resulting aqueous phase concentrations. For instance, the two-component (TCE:HEX) column system produced initial aqueous phase TCE concentrations of approximately 325 mg/L due to the initial TCE mole fraction (0.2) in the NAPL; whereas the TCE:HEX batch system resulted in equilibrium TCE concentrations of approximately 337 mg/L. The column study used initial TCE:HEX NAPL mole fraction (0.2:0.8) to obtain total moles injected into the column (see eq. 4). The batch study also implemented the same method to evaluate total moles of the system, determined directly by mole fraction (see eq. 4). Thus, applying the ideal form of Raoult's Law for the batch experiments produced an equilibrium aqueous TCE concentration prediction of 240 mg/L ($x_{\text{TCE}} = 0.2$; $C_S = 1,200$ mg/L). Since aqueous TCE concentrations equilibrated around 337 mg/L (average), nonideal NAPL mixture dissolution could be accounted for by incorporating a NAPL phase activity coefficient ($\gamma_{\text{TCE}}^{\text{N}}$) of 1.4. This activity coefficient is about half that of the column-calibrated activity coefficient ($\gamma_{\text{TCE}}^{\text{N}} = 2.68$), which suggests that kinetically controlled mass transfer limitations may be occurring during the dynamic flushing experiments and/or that as mole fraction of TCE (target contaminant) decreases significantly, nonideality effects become enhanced.

By comparing the results of the differing mole fraction scenarios (i.e. 0.2:0.8 vs. 0.003:0.997) it is immediately evident that not only do structural differences between components within a multi-component system affect nonideality, the variance between divergent mole

fractions also increases nonideality. As seen in the 0.2:0.8 mole fraction batch experiment (Fig. 11), equilibrium conditions were achieved at 337 mg/L (average), but Raoult's law (Eq 1) predicted an aqueous concentration of 240 mg/L. Comparison of these values (Eq. 6) results in an activity coefficient ($\gamma_{\text{TCE}}^{\text{N}}$) of 1.4. Next, comparison of the 0.003:0.997 mole fraction NAPL solution yielded an equilibrium aqueous concentration of 22.3 mg/L whereas Raoult's law predicted an aqueous concentration of 3.6 mg/L. The calculated activity coefficient, $\gamma_{\text{TCE}}^{\text{N}}$, (i.e. degree of dissolution nonideality) for this system was 6.1 (Eq. 6) was significantly greater than the less disparate mole fraction system (0.2:0.8). With both systems incorporating the same compounds (TCE and n-hexadecane) the degree of nonideality must be related, in part, to the differing degrees of mole fractions. Thus, mole fraction differences also influence the degree of nonideality for dissolution behavior. More specifically, as mole fraction decreases, the degree of nonideality increases.

It is interesting to note that batch studies conducted by McCray and Dugan (2002) showed that NAPL phase activity coefficients ($\gamma_{\text{TCE}}^{\text{N}}$) approached 6 at TCE mole fractions (x_{TCE}) of 0.0001 for TCE:Decane (TCE:DEC) NAPL mixture systems. From their work, extrapolated values for a TCE mole fraction of 0.2 resulted in a measured TCE concentration of approximately 300 mg/L, which was about 1.25 times greater than that predicted by Raoult's Law. Therefore, this previous study which investigated a range of TCE mole fractions (0.1 to 0.0001) within n-decane ($\text{C}_{10}\text{H}_{22}$), demonstrated that nonideality for a 0.2 TCE mole fraction was about 1.25 ($\gamma_{\text{TCE}}^{\text{N}} = 1.25$). From previous discussions relating nonideal dissolution to differences in chemical molecular structure and dissimilarity, and the longer chained n-hexadecane ($\text{C}_{16}\text{H}_{34}$) used in the experiments of this study, it is expected that the nonideality (between TCE and HEX)

would be greater than the TCE:DEC system used in McCray and Dugan (2002). Considering that n-hexadecane and n-decane are both n-alkanes with chain/link structures, the importance of these additional atoms appears to directly influence the NAPL mixture's degree of nonideality.

CHAPTER 4: Conclusion

Contamination of soil and groundwater by nonaqueous phase liquids (NAPLs) poses serious risks to human health and the environment and present major challenges for cleanup. The presence of complex NAPL mixtures in the subsurface further complicates remediation efforts, transport predictions, and the development of accurate risk assessments. NAPL distribution (pools and residual saturation conditions), NAPL composition-dependent factors (mole-fraction and solubility), limited NAPL-water surface area and limited hydraulic accessibility (bypass/preferential flow), and low residence time can contribute to rate-limited dissolution of the NAPL. This study evaluated the importance of 1) distribution of NAPL (uniform vs. non-uniform), 2) NAPL- water interfacial surface area (constant vs. changing), 3) multi-component NAPLs (mole fraction dependence), and 4) intra-NAPL diffusion on NAPL dissolution and target contaminant (TCE) aqueous phase concentrations. As NAPL composition and distribution are typically highly variable at most contamination sites, it was the purpose of this study to assess the effects of the above variables on resulting aqueous phase contaminant concentrations and removal (by dissolution) and elucidate how this can impact real world sites. A series of comprehensive column and sequential batch experiments allowed for a detailed characterization and quantification of NAPL dissolution behavior under various conditions. Significant differences in elution behavior and mass removal effectiveness were observed for the various systems tested. A set of multi-component NAPL dissolution experiments (TCE: Hexadecane)

with varying mole fractions allowed for the determination of the degree of dissolution nonideality and the influence of NAPL interfacial area on dissolution behavior. In addition, these experiments provided an improved understanding of the primary factors controlling NAPL dissolution processes and how this affects resulting aqueous phase concentrations for the simple-two-component NAPL mixtures.

Under uniform (“homogeneous”) NAPL distribution conditions, single component NAPL (TCE) dissolution occurs in three distinct phases: 1) steady state dissolution where there is sufficient NAPL present to maintain maximum solubility conditions, 2) rapid decline in aqueous-phase concentration, where a critical point is achieved when there is insufficient NAPL present to maintain maximum solubility conditions, and 3) concentration tailing effects where effective dissolution has been exhausted and NAPL removal efficiency is minimal. This type of NAPL dissolution behavior results as a function of changing NAPL-water interfacial surface area. Since NAPL removal results from mass entering the aqueous phase, the actual volume (interfacial area) of the NAPL body decreases as dissolution proceeds. This type of dissolution is considered the least effective as it requires a great deal of solvent (in this case water) to remove NAPL mass from the system. Steady state conditions tend to persist for an extended period of time as mass flux is maximized due to an initial sufficient NAPL mass (volume and interfacial area) available to maintain maximum aqueous phase concentrations (i.e. solubility). Tailing effect concentrations are often orders of magnitude greater than enforceable regulatory concentration standards, thus, reducing aqueous contaminant concentrations to (or below) regulatory drinking water limits (maximum contaminant levels - MCLs) has proven to be extremely difficult if not impossible to achieve, requiring impractical flushing volumes and time

periods to meet such goals (decades to centuries). This tailing can persist indefinitely, which may require additional remediation in order to meet acceptable regulatory standards.

Non-uniform (“Heterogeneous”) NAPL distribution conditions are typical at most real world contamination sites, which exemplifies the need for further study as conducted herein. NAPLs tend to collect in the most receptive areas leading to non-uniform NAPL distributions (i.e. pools, etc.), which can limit flushing accessibility and dissolution. In order to create non-uniform NAPL distributions (i.e. “pooling”) in the column system, porous medium packing methods were conducted in a way to establish variation in pore size arrangement. Hence, it was intended that during injection of NAPL into the column, preferential zones would be established with NAPL creating an overall non-uniform distribution. Upon achieving these conditions, we were able to observe the resulting contaminant (TCE) dissolution/elution behavior. The overall TCE elution behavior was similar to the single-component TCE uniform distribution experiment, however, dissolution —shouldering, exhibited by multiple stages of steady-state phase dissolution (elution) and much longer flushing times required to deplete the NAPL mass, was observed for this experiment. Dissolution occurred in five phases: 1) steady state dissolution where there was sufficient NAPL present to maintain maximum solubility conditions, 2) rapid decline in aqueous-phase concentration, where a critical point is achieved when there is insufficient NAPL present to maintain maximum solubility conditions, 3) secondary steady state phase where —pooled NAPL (initially less accessible fraction) allows for aqueous concentrations to be maintained at lower constant value, 4) secondary rapid decline of aqueous-phase concentration where NAPL mass is insufficient to maintain steady-state elution, and 5) concentration tailing effects where effective dissolution has been exhausted and NAPL removal efficiency is minimal. This type of NAPL dissolution behavior is comparable to the uniform

conditions as removal efficiency is minimal. More importantly, it can be considered less efficient as it requires much more flushing in order to achieve the same removal results. Consequently, the importance of changing (variation) interfacial surface area due to NAPL distribution was clearly evident. As dissolution occurs, available NAPL surface area decreases, but with this system, non-uniform distribution of NAPL (i.e. pools or high saturation zones) demonstrates the importance of interfacial surface area variation effects on resulting dissolution behavior. During flushing conditions, once a critical point is achieved where there is insufficient NAPL present in the system, rapid declines in aqueous-phase contaminant concentration will occur until concentration tailing effects are observed. For the non-uniform NAPL (TCE) distribution experiment, the initial steady-state elution (dissolution) phase (i.e. at solubility limit) is maintained as a result of sufficient NAPL mass (volume and interfacial area) and hydraulic accessibility. However, as this initial hydraulically accessible mass is reduced, a rapid decline in aqueous-phase concentration occurs until a second, lower concentration, steady-state elution phase results. This second steady-state phase is likely occurs at a point where initially —inaccessible! TCE-NAPL mass becomes accessible or in large enough amounts (enough volume or interfacial area) to maintain constant concentration for a period of flushing. At a point where insufficient NAPL mass (reduction of interfacial area) exists, TCE concentrations rapidly decline until ineffective removal occurs and observed concentration tailing results. At most real-world contamination sites, non-uniform (—heterogeneous!) NAPL contaminant distribution is expected and typically observed. Thus, dissolution behavior can vary by location; however, the conditions under which a NAPL is subjected directly influences its distribution and subsequent dissolution. The simplified single-component NAPL scenarios (uniform vs. non-uniform distribution) presented in this study demonstrate how subsurface heterogeneity can influence

NAPL distribution (i.e. pools and variations in NAPL saturations) and resulting dissolution (elution) behavior, significantly controlling and limiting the effectiveness of field-scale remediation goals.

Many of the sites contaminated by NAPL, throughout the U.S. and world, exist as complex multi-component chemical mixtures (i.e. multi-component NAPLs). Hazardous waste disposal facilities comprise a wide variety of contaminants which incorporate many different types of chemicals. As a result, if a site is subject to leakage, multiple contaminants can be introduced into the subsurface. Consequently, it is not only important to understand a single-component NAPL dissolution behavior but also multi-component NAPL dissolution behavior as a function of the individual properties of each component of the bulk NAPL present. The purpose of this part of the study was to evaluate the importance of constant versus changing NAPL interfacial surface area on dissolution processes during water flushing conditions. A two-component NAPL mixture was created whereby the bulk of the NAPL consisted of an insoluble component (Hexadecane). In this way, the NAPL-water interfacial area would remain constant during water flushing and the resulting target contaminant (TCE) dissolution could be evaluated independent of changing NAPL interfacial area, and subsequently compared to the single-component NAPL (TCE) experiments whereby NAPL interfacial area is reduced, as dissolution proceeds. A 1:14 volume fraction (0.2:0.8 mole fraction) of TCE: Hexadecane was chosen as the representative multi-component NAPL mixture. The dissolution behavior of TCE from the multi-component NAPL system exhibited significantly different behavior than the single-component NAPL dissolution experiments. The dissolution (elution) behavior occurred in two stages: 1) extremely brief (minimal) steady-state elution period, as initial TCE concentrations were analogous to predicted equilibrium values, and 2) relatively constant decline in aqueous-phase

concentrations (constant dissolution rate) without the presence of a concentration tailing phase. This observed behavior suggests that intra-NAPL diffusion of TCE within the bulk NAPL (to the NAPL boundary surface) was relatively constant during the flushing period. Sequential batch TCE dissolution experiments for the both single-component NAPL (TCE) and the multi-component NAPL (TCE:HEX) showed nearly identical dissolution rates, further indicating that TCE intra-NAPL diffusion was not rate limited for the systems investigated in these studies. The potentially constant intra-NAPL diffusion rate and the constant NAPL surface area of the multi-component NAPL system (TCE:HEX) produced a constant decline in aqueous phase TCE concentration during the entire duration of flushing, indicating a constant dissolution rate over time. This indicates that potentially for some compounds within complex NAPL mixtures, constant removal can be expected without major rate limiting behavior. Therefore, characterization of NAPL contamination mixtures at real-world sites is critical to appropriately predict the removal of particular target compounds during remediation processes.

For sites contaminated by multi-component NAPLs, remediation approaches typically incorporate mole fraction estimates in order to predict the dissolution and removal of individual constituents within the bulk NAPL utilizing Raoult's Law (Eq. 1). The purpose of this part of the study was to evaluate and understand the influence of mole fraction on the dissolution behavior and whether these systems effectively be described by equilibrium dissolution processes. Dissolution ideality or nonideality can be quantified by the organic-phase (NAPL) activity coefficient (γ^N). The degree of dissolution nonideality can be described by greater deviation of NAPL activity coefficients from unity (i.e. larger values of $\gamma^N > 1$, in this case). As expected from previous studies, the TCE: Hexadecane NAPL solutions investigated herein resulted in nonideal dissolution behavior. The batch experiments incorporating the larger TCE mole fraction NAPL

mixtures (TCE:HEX 0.2:0.8) resulted in activity coefficients (γ^{TCE}) that were above unity at approximately 1.7. This dissolution nonideality behavior was attributed in part to the mole fraction disparity and dissimilarities in molecular structure. Furthermore, in order to understand mole fraction dependencies on dissolution behavior, a 1:1000 volume fraction TCE:HEX NAPL mixture (0.003:0.997 mole fraction) was also used for the equilibrium dissolution batch experiments. This experiment was conducted to determine the influence of varying the mole (i.e. decreasing the target TCE contaminant mole fraction) on dissolution nonideality as quantified by the NAPL-phase (TCE) activity coefficient. It was hypothesized that with greater increase in mole fraction ratio (TCE:HEX 0.003:0.997), greater nonideal dissolution effects would be experienced for TCE. The results of these batch experiments showed greater dissolution nonideality as observed by the higher calculated NAPL-phase activity coefficient (γ^{TCE}) of 6.1. These studies indicated that dissolution nonideality increases as the mole fraction ratio increases for a given contaminant NAPL mixture system.

Comparison of dissolution rates observed during the sequential batch (equilibrium) experiments demonstrated that dissolution of TCE remains constant regardless of the initial mole fraction present (Table 6). This behavior suggests that the rate of intra-NAPL diffusion was also constant over the duration of the experiments and that intra-NAPL diffusion was not a limiting factor on the rate of multi-component dissolution under the conditions of these experiments. By evaluating the rates of dissolution of TCE into the aqueous phase, more accurate risk assessments can be conducted in order to predict dissolution behavior. Multi-component NAPL systems are prevalent at many contaminated sites and understanding dissolution processes and the conditions which may result in constant dissolution rates is critical for predicting contaminant transport and designing effective remediation strategies. The results of this study

indicate that for particular compounds of interest where the bulk of the NAPL is characterized as insoluble, dissolution rates of target species may be independent of respective mole fraction and can provide invaluable insight for evaluating cleanup times.

Due to the variables isolated for each experimental condition, mass removal behavior was characterized for each scenario. While the TCE:HEX system resulted in the fastest removal time (least pore volumes flushed) its removal behavior was not considered to be the most efficient in terms of mass flux reduction per mass removed. Mass flux was immediately reduced upon induced flushing. This behavior was likely associated with the significantly lower TCE mass available within the multi-component NAPL systems (TCE:HEX mole fraction 0.2:0.8) compared to the single-component TCE systems. In addition, the fractional mass ratio removed would therefore be impacted greatest within the system containing overall less target compound mass. The uniform NAPL-TCE distributed system (TCE-U1) experienced optimal mass removal efficiency in terms of mass flux reduction analysis whereby mass flux remained high until nearly all of the TCE mass was depleted. In terms of normalized TCE mass recovery, the TCE-U1 experiment produced the second best results, removing the mass in a relatively short period of time. The non-uniform NAPL distributed systems (TCE-NU1) experienced relatively inefficient mass removal in comparison to the mass removal for the uniform TCE NAPL system based on mass flux reduction analysis. Maximum high mass flux is maintained initially but after about 60% of the TCE mass is removed, mass flux is significantly reduced and variable until most of the mass was depleted.

Comprehensive laboratory studies, such as that presented herein, provide the ability to isolate and evaluate specific variables to examine and understand particular processes controlling

NAPL dissolution behavior. This study provided an improved understanding of NAPL dissolution processes as a function of NAPL distribution, NAPL-composition, and NAPL interfacial-surface area. Evaluation of these processes provided the ability to assess which systems would result in efficient mass removal relationships and those that would be limited by rate-limited mass transfer (interfacial area changes, bypass/preferential flow) and nonideal dissolution effects (i.e. mole fraction, chemical dissimilarity). For the systems investigated in this study, Raoult's Law generally under-predicted aqueous-phase TCE concentrations for the multi-component NAPL dissolution flushing experiments, likely due to a combination of factors including rate-limited mass-transfer effects, mole fraction composition, and differences between chemical molecular structure. However, these experiments suggest that, for particular compounds of a NAPL mixture, the rate of compound dissolution rate may be independent of mole fraction. The results of this study have valuable potential and promise for applications at the field scale. Detailed characterization of NAPL mixtures obtained from a contaminated field site can be used to make better predictions of resulting aqueous phase concentrations (accounting for dissolution nonideality) allowing for more accurate risk assessments and contaminant transport predictions, and the development of more effective remediation strategies.

References

- Anderson, Michael R.; Johnson, Richard L.; Pankow, and James F., 1992 Dissolution of dense chlorinated solvents into ground water; 1, Dissolution from a Well-defined residual source *Ground Water*, 30(2):250-256
- Bai, M.; Elsworth, D.; Inyang, H. I.; and Roegiers, J.C., 1997. Modeling contaminant migration with linear sorption in strongly heterogeneous media. *Journal of Environmental Engineering*, 123(11):1116-1125
- Banerjee, S., 1984, Solubility of organic mixtures in Water, *Environmental Science Technology*. 18 (8), 587-597
- Borden, Robert C. and Pivoni, Marvin D., 1992. Hydrocarbon dissolution and transport; a comparison of equilibrium and kinetic models. *Journal of Contaminant Hydrology*, 10(4):309-323
- Boving, T.B., and Brusseau, M.L. 2000. Solubilization and removal of residual Trichloroethene from porous media: Comparison of several solubilization agents. *Journal of Contaminant Hydrology*, 42, 51-67.
- Brahma, Priti P. and Harmon, Thomas C., 2003. The effect of multi-component diffusion on NAPL dissolution from spherical ternary mixtures. *Journal of Contaminant Hydrology*, 67(1-4):43-60
- Broholm, K., Feenstra, S., 1995. Laboratory measurements of the aqueous solubility of mixtures of chlorinated solvents. *Environ. Toxicol. Chem.* 14 (1), 9 –15
- Brown, D. G., C. D. Knightes, and C. A. Peters, 1999. Risk assessment for polycyclic aromatic hydrocarbon NAPLs using component fractions, *Environ.Sci. Technol.*, 33(24), 4357–4363
- Brusseau, M.L., Zhang, Z., Nelson, N.T., Cain, R.B., Tick, G.R., and Oostrom, M. 2002. Dissolution of non-uniformly distributed immiscible liquid: Intermediate-scale experiments and mathematical modeling. *Environ. Sci. Technol.*, 36, 1033-1041.

- Brusseau, M.L., DiFilippo, E.L., Marble, J.C., Oostrom, M., 2008. Mass removal and mass flux reduction behavior for idealized source zones with hydraulically poorly –accessible immiscible liquid. *Chemosphere*. 71, 1551-1521
- Burris, D. R., and W. G. MacIntyre, 1985. Water solubility behavior of binary hydrocarbon mixtures, *Environ. Toxicol. Chem.*, 4, 371– 377
- Carroll, K. C., 2007. Characterization, Dissolution, and Enhanced Solubilization of Multi-component Non-Aqueous Phase Liquid in Porous Media. A Dissertation Submitted to the Faculty of the Department of Hydrology and Water Resources, University of Arizona
- Carroll, K.C. and Brusseau, M.L. Dissolution, Cyclodextrin-enhanced Solubilization, and Mass Removal of an Ideal Multicomponent Organic Liquid. *Journal of Contaminant Hydrology*, 106(1-2): 62-72, 2009.
- DiFilippo, E.L. and Brusseau, M.L. 2008. Relationship between mass-flux reduction and source-zone mass removal: Analysis of field data *Journal of Contaminant Hydrology*, 98(1-2):22-35
- Enfield, Carl G., Wood, A. Lynn , Brooks, Michael C. and Annable, Michael D. 2002 Interpreting tracer data to forecast remedial performance (*in* Groundwater quality; natural and enhanced restoration of groundwater pollution) *IAHS-AISH Publication*, 275 11-16
- Falta, Ronald W., Bulsara, Nimesha, Henderson, James K. and Mayer, Richard A., 2005. Leaded-gasoline additives still contaminate ground water. *Environmental Science & Technology*, *ES & T*, 39(18):378A-384A
- Frind, E.O., Molson, J.W., Schirmer, M., Guiguer, N., 1999. Dissolution and mass transfer of multiple organics under field conditions: the Borden emplaced source. *Water Resour. Res.* 35 (3), 683– 694
- Geller, J. T. and Hunt, J. R., 1993. Mass transfer from nonaqueous phase organic liquids in water-saturated porous media. *Water Resources Research*, 29(4):833-845
- Haebeck, M., 1994. Toxicological Profile for Toluene. Agency for Toxic Substances and Disease Registry: United States Public Health Service
- Hinlein, E. S., 1999. Bioventing and biosparging at a site contaminated with JP-4 and TCE, Ph.D. dissertation, 523 pp., Univ. of Mass., Amherst
- Illangasekare, Tissa H., Ramsey (Jr.), James L., Jensen, Karsten H., Butts, Michael B., 1995. Experimental study of movement and distribution of dense organic contaminants in heterogeneous aquifers *Journal of Contaminant Hydrology*, 20, (1-25)

- Imhoff, Paul T., Jaffe, Peter R., and Pinder, George F., 1994. An experimental study of complete dissolution of a nonaqueous phase liquid in saturated porous media, *Water Resources Research*, 30(2):307-320
- Jawitz, J. W., M. D. Annable, P. S. C. Rao, and D. Rhue, 1998. Field implementation of a Winsor-type 1 surfactant/alcohol mixture for in situ solubilization of a complex LNAPL as a single-phase microemulsion, *Environ.Sci. Technol.*, 32(4), 523– 530
- Jawitz, J. W., Fure, A. D., Demmy, G. G., Berglund, S. and Rao, P. S. C., 2005. Groundwater contaminant flux reduction resulting from nonaqueous phase liquid mass reduction *Water Resources Research*, 41(10)
- Kueper, Bernard H. and Frind, Emil O., 1988. An overview of immiscible fingering in porous media. *Journal of Contaminant Hydrology*, 2(2):95-110
- Lesage, S., and S. Brown, 1994. Observation of the dissolution of NAPL mixtures, *J. Contam. Hydrol.*, 15, 57– 71
- Marble, J.C. , DiFilippo, E.L., Zhang, Z., Tick, G.R. and Brusseau, M.L., 2008. Application of a lumped-process mathematical model to dissolution of non-uniformly distributed immiscible liquid in heterogeneous porous media. *Journal of Contaminant Hydrology*, 100(1-2):1-10
- McCray, J. E., and M. L. Brusseau, 1999. Enhanced in-situ flushing of multiple component immiscible organic liquid contamination at the field scale using cyclodextrin: Mass-transfer phenomena, *Environ. Sci. Technol.*, 33(1), 89– 95.
- McCray, J.E., and Dugan P.J., 2002, Non-ideal equilibrium dissolution of trichloroethene from a decane-based nonaqueous phase liquid mixture: Experimental and modeling investigation. *WATER RESOURCES RESEARCH*, VOL. 38, NO. 7, 1097
- McCray, J.E., Tick, G. R., Jawitz, J. W., Gierke, J. S., Brusseau, M. L., Falta, R. W., Knox, R.C., Sabatini, D. A., Annable, M. D., Harwell, J. H., Wood, A. L., 2011. Remediation of NAPL Source Zones: Lessons Learned from Field Studies at Hill and Dover AFB. *Ground Water*
- Mercer, J.W., Choen, R.M. 1990. A review of immiscible fluids in the subsurface: Properties, models, characterization and remediation. *J. Contam. Hydrol.*, 54, 174-193.
- Miller, C.T., Poirier-McNeill, M.M., Mayer, A.S., 1990. Dissolution of trapped nonaqueous phase liquids-mass transfer characteristics. *Water Resour. Res.* 26 (11), 2783– 2796.
- National Research Council (NRC) (U.S.). 1999. *Groundwater and Soil Cleanup: Improving Management of Persistent Contaminants*. Washington, DC: National Academy of Sciences.

- National Research Council (NRC) (U.S.). 2000. *Research Needs in Subsurface Science*. Washington, DC: National Academy of Sciences
- National Research Council (NRC) (U.S.). 2005. *Contaminants in the Subsurface: Source Zone Assessment and Remediation*. Washington, DC: National Academy of Sciences.
- OMB Watch. 2011. Despite delays and threats, EPA finally classifies TCE as a cancer-causing chemical. 11878
- Pankow, J.F., Cherry, J.A. (eds.) 1996. Dense chlorinated solvents and other DNAPLs in groundwater. Portland, Oregon: Waterloo Press.
- Parker, J. C., and Park, E. _2004_. —Modeling field-scale dense nonaqueous phase liquid dissolution kinetics in heterogeneous aquifers. *Water Resour. Res.*, 40_5_, W05109
- Pennell, K. D., Abriola, L. M., and Weber, W. J. _1993_. —Surfactant enhanced solubilization of residual dodecane in soil columns. 1. Experimental investigation. *Environ. Sci. Technol.*, 27_12_, 2332–2340
- Powers, S. E., Abriola, L. M., and Weber, W. J. _1992_. —An experimental investigation of nonaqueous phase liquid dissolution in saturated subsurface systems: Steady-state mass transfer rates. *Water Resour. Res.*, 28_10_, 2691–2705.
- Powers, S. E., Abriola, L. M., and Weber, W. J. _1994_. —An experimental investigation of nonaqueous phase liquid dissolution in saturated subsurface systems—Transient mass-transfer rates. *Water Resour. Res.*, 30_2_, 321–332.
- Rao, P.S.C., M.D. Annable, R.K. Sillan, D. Dai, K. Hatfield, W.D. Graham, A.L. Wood, and C.G. Enfield. 1997. Field scale evaluation of in situ cosolvent flushing for enhanced aquifer remediation. *Water Resources Research* 33, no. 12: 2673–2686.
- Rao, P. S. C., Kim, Heonki and Annable, Michael D., 2002. (in *Methods of soil analysis; Part 4, Physical methods*) *Soil Science Society of America Book Series*, 5 783-796
- Schwartz, Franklin W. and Zhang, Hubao, 2003. *Fundamentals of ground water* John Wiley & Sons, New York, NY, United States, pp 583
- Schwarzenbach, R. P. P. M. Gschwend, and Imboden, D. M., 1993. *Environmental Organic Chemistry*, Wiley Interscience, New York,
- Seagren, E. A., Rittman, B. E. and Valocchi, A. J. 1999. A critical evaluation of the local-equilibrium assumption in modeling NAPL-pool dissolution, *J. Contam. Hydrol.*, 39(1), 109– 135

- Skubal, K. L., Barcelona, M. J. and Adriaens, P. 2001. An assessment of natural biotransformation of petroleum hydrocarbons and chlorinated solvents at an aquifer plume intersect, *J. Contam. Hydrol.*, 49(1-2), 151– 170
- Soga, K., Page, J. W. E., and Illangasekare, T. H. _2004_. —A review of NAPL source zone remediation efficiency and the mass flux approach. *J. Hazard. Mater.*, 110,1–3, 13–27
- Tick, G.R., and Rincon, E.A., 2009. Effect of Enhanced-Solubilization Agents on Dissolution Mass Flux from Uniformly Distributed Immiscible-Liquid Trichloroethene (TCE) in Homogeneous Porous Media. *Water Air and Soil Pollution*, 204:315-332, 10.1007/s11270-009-0047-3.
- Tick, G.R., Lourenso, F., Wood, A.L. and Brusseau, M.L., 2003. Pilot-scale demonstration of cyclodextrin as a solubility-enhancement agent for the remediation of a tetrachloroethene-contaminated aquifer. *Environmental Science & Technology* 37, no. 24: 5829–5834
- Van Genuchten, M.T., 1981. CFITIM Model: Estimates parameters in several equilibrium and non-equilibrium transport models from solute breakthrough curves. Research Report No. 119, USDA Salinity Laboratory, Riverside, CA.
- Werner, D., Karapanagioti, H.K., Hohener, P., 2009. Diffusive partitioning tracer test for the quantification of nonaqueous phase liquid (NAPL) in the vadose zone: Performance evaluation for heterogeneous NAPL distribution. *Journal of Contaminant Hydrology*, 108, 54-63
- Wilson, W. E., Moore, J. E. (1998). American Geological Institute: Glossary of Hydrogeology, American Geological Institute, Alexandria, VA.
- Wright, D. Johnson, Pedit, J.A., Gasda, S.E., Farthing, M.W., Murphy, L.L., Knight, S.R., Brubaker, G.R., Miller, C.T., 2010. Dense, viscous brine behavior in heterogeneous porous medium systems, *Journal of Contaminant Hydrology*, 115, 1-4
- Yu, J.-J., and Chou, S.-Y., 2000. Contaminated site remedial investigation and feasibility removal of chlorinated volatile organic compounds from groundwater by activated carbon fiber adsorption, *Chemosphere*, 41(3), 371– 378
- Zemo, D.A., Graf, T. E., Bruya, J. E. (1993). The importance and benefit of fingerprint characterization in site investigation and remediation focusing on petroleum hydrocarbons. Proc of Petroleum Hydrocarbons and Organic Chemicals in Ground Water: Prevention, Detection, and Restoration. National Ground Water Assoc. Columbus, OH, p. 39-54

Zhang, Z., Brusseau, M.L., (1999). Non-ideal transport of reactive solutes in heterogeneous porous media 5. Simulating regional-scale behavior of a trichloroethene plume during pump and-treat remediation. *Water Resources Research*. Vol. 35, No. 10, 2921-2935.

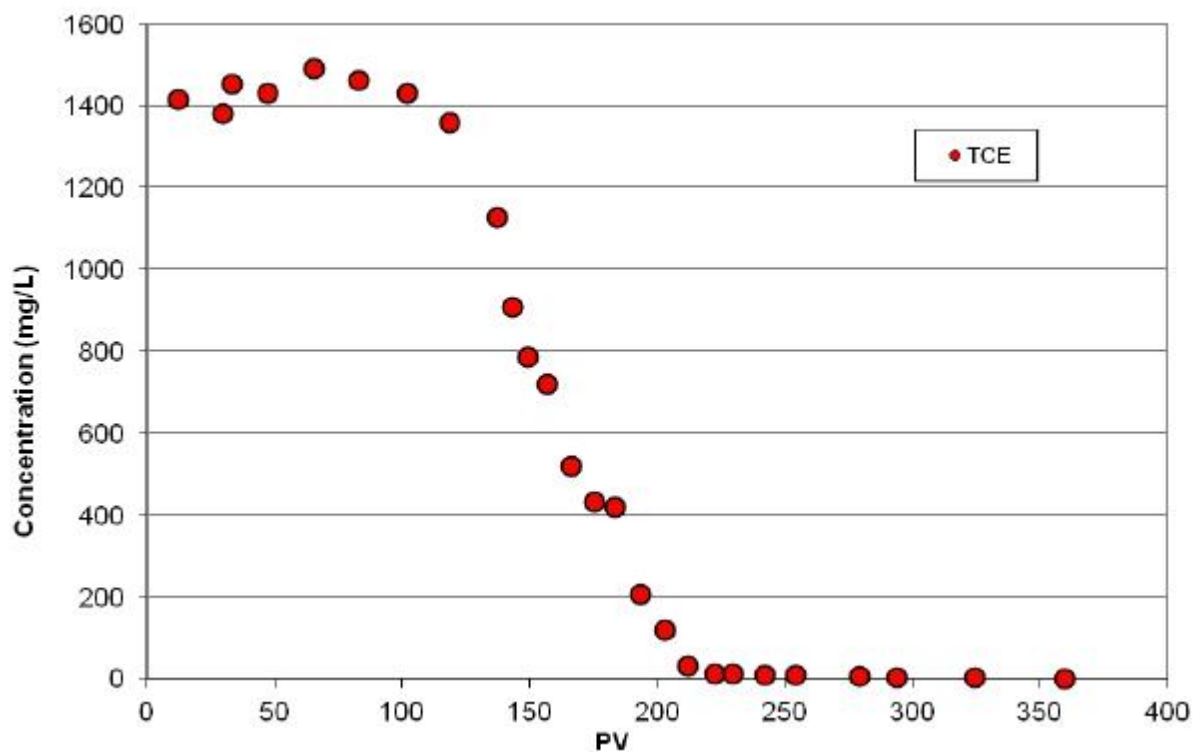
Zhang, C., Werth, C.J., and Webb, A.G., 2007. Characterization of NAPL source zone architecture and dissolution kinetics in heterogeneous porous media using magnetic resonance imaging. *Environmental Science Technology*, 41, 3672-3678

Zhu, Jianting and Sykes, Jonathan F., 2004. Simple screening models of NAPL dissolution in the subsurface, *Journal of Contaminant Hydrology*, 72(1-4):245-258

APPENDIX A

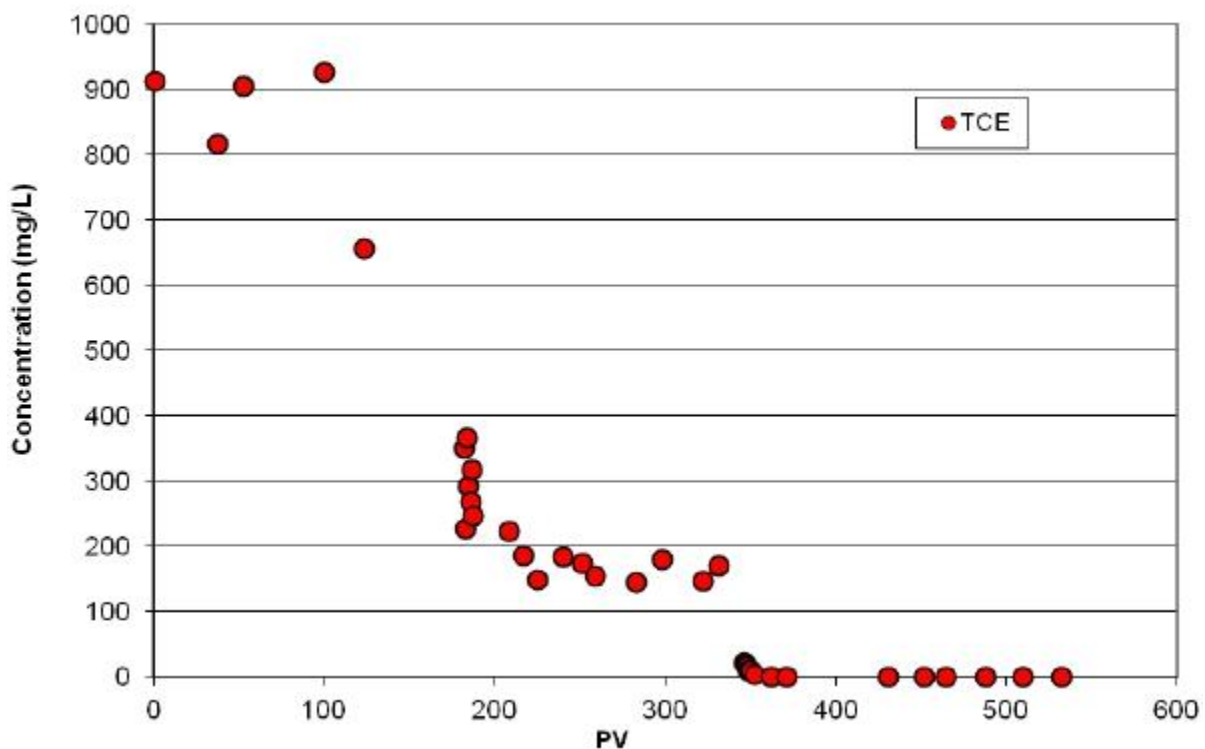
REPLICA DATA

TCE Elution vs. Pore Volume

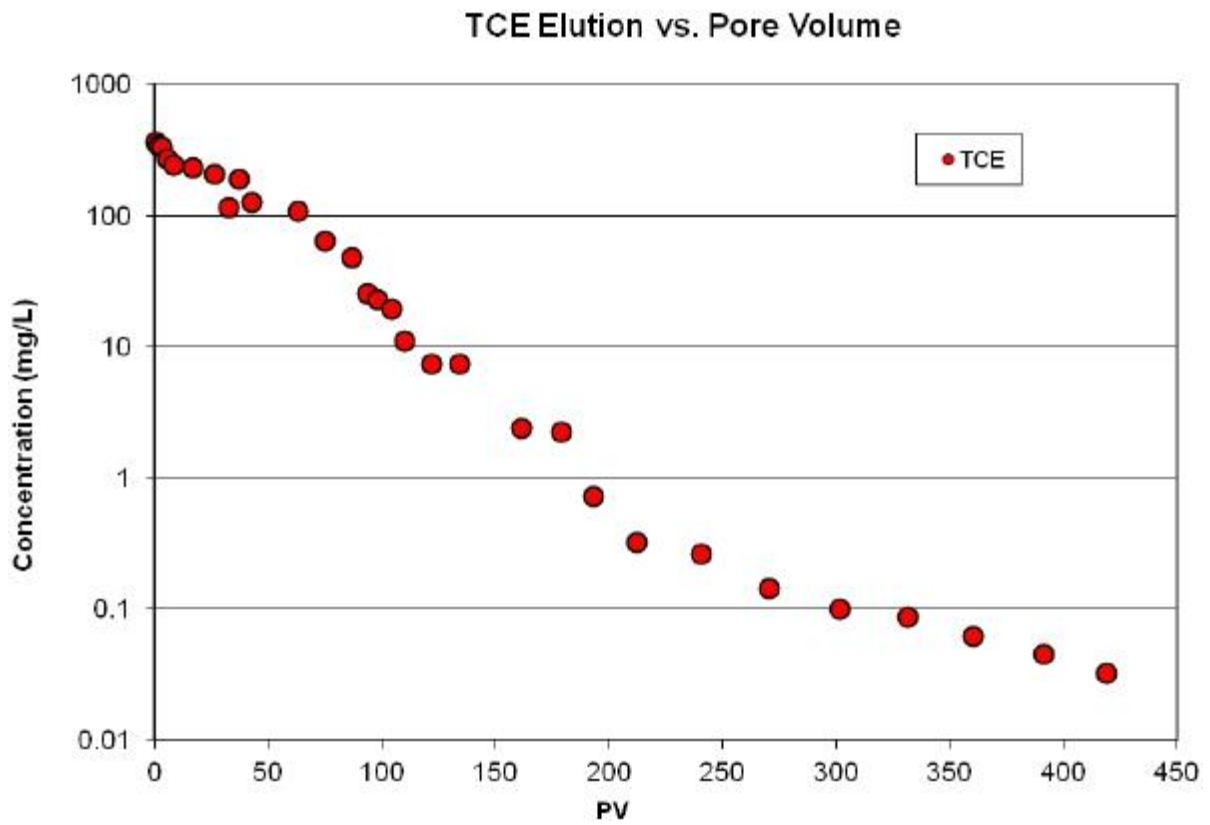


Replica Data – Gas Chromatograph: TCE elution curve [TCE-U1] under uniformly packed conditions

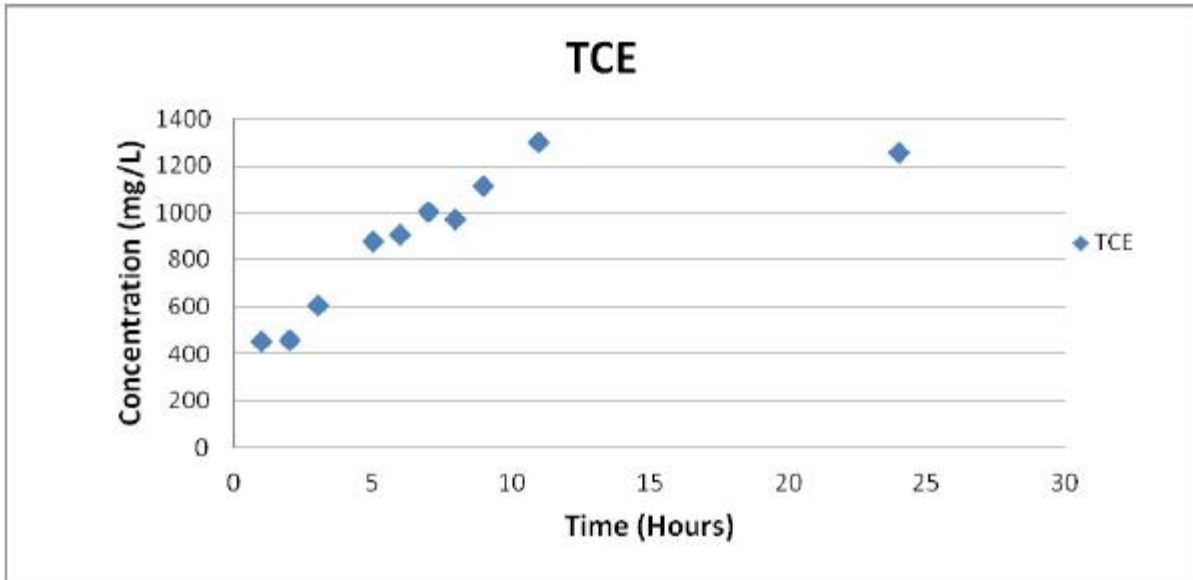
TCE Elution vs. Pore Volume



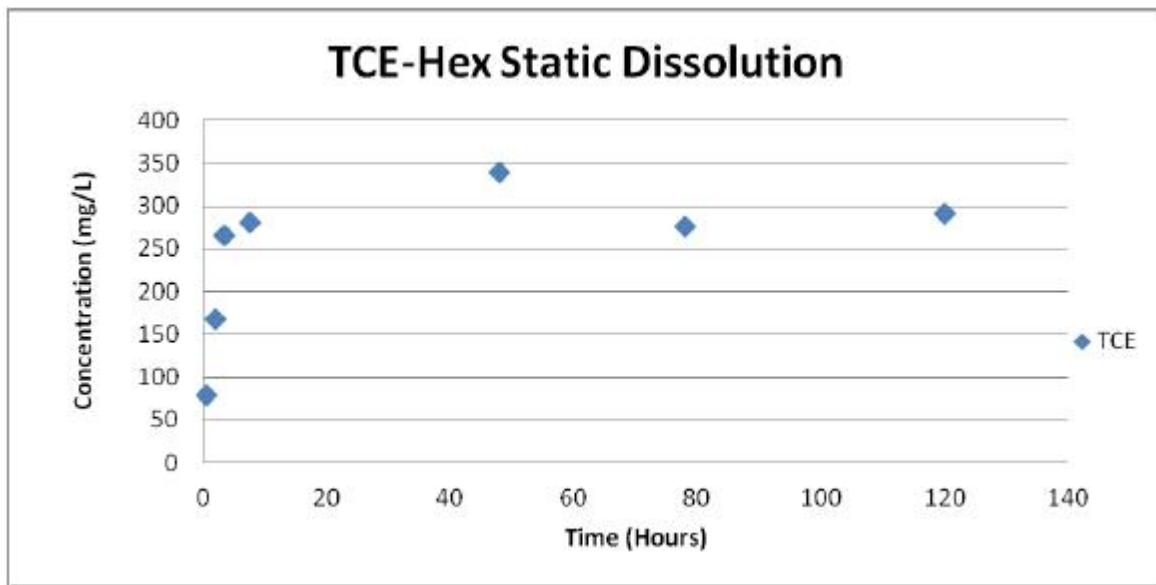
Replica Data- Gas Chromatograph: TCE elution [TCE-NU1] curve under non-uniformly packed conditions



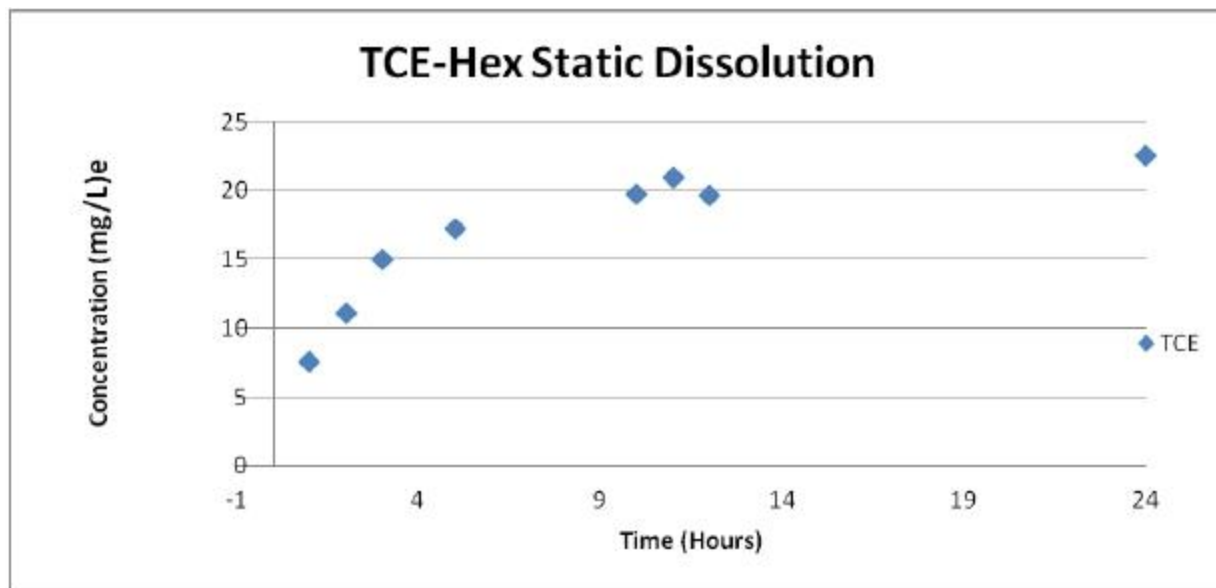
Replica Data – Gas Chromatograph: TCE elution curve under uniformly packed conditions for the two-component TCE:Hexadecane NAPL system



Replica Data – TCE – B2: NAPL-TCE equilibrium time-series batch dissolution experiments



Replica Data – TH –B2: NAPL-TCE:Hexadecane (1:14 volume fraction; 0.2:0.8 mole fraction) equilibrium time-series batch dissolution experiment



Replica Data – TH – B2: NAPL-TCE:Hexadecane (1:1000 volume fraction; 0.003:0.997 mole fraction) equilibrium time-series batch dissolution experiments